Published in Geophysical Journal International 158 : 753-774, 2004,
which should be used for any reference to this work

Present-day geodynamics in the bend of the western and central Alps as constrained by earthquake analysis

Bastien Delacou,* Christian Sue, Jean-Daniel Champagnac and Martin Burkhard
Institut de Géologie, Université de Neuchâtel, Switzerland

Accepted 2004 March 26. Received 2004 March 3; in original form 2003 May 28

SUMMARY

The contrasted tectonics of the western/central Alps is examined using a synthesis of 389 reliable focal mechanisms. The present-day strain regime is mapped and interpolated for the entire Alpine belt based on a newly developed method of regionalization. The most striking feature is a continuous area of extension which closely follows the large-scale topographic crest line of the Alpine arc. Thrusting is observed locally, limited to areas near the border of the Alpine chain. A majority of earthquakes within the Alps and its forelands are in strike-slip mode. Stress inversion methods have been applied to homogenous subsets of focal plane mechanisms in order to map regional variations in stress orientation. The stress state is confirmed to be orogen-perpendicular both for σ_3 in the inner extensional zones and σ_1 in the outer transcurrent/transpressional zones. Extensional areas are well correlated with the part of the belt which presents the thickest crust, as shown by the comparison with the Bouguer anomaly and the average topography of the belt. In the northwestern Swiss Alps, extension is also correlated with currently uplifting zones. These observations and our strain/stress analyses support a geodynamic model for the western Alps in which the current activity is mostly a result of gravitational 'body' forces. Earthquakes do not provide any direct evidence for ongoing convergence in the Alpine system, but a relationship with ongoing activity of complex block rotations of the Apulian microplate cannot be ruled out.

Key words: active tectonics, buoyancy forces, earthquake focal mechanisms, orogen-perpendicular extension, stress inversion, western/central Alps.

1 INTRODUCTION AND TECTONIC SETTING

The Alpine belt resulted from the Tertiary convergence between the European and African plates. The Apulian microplate was caught in between the two, leading to the closure of the mid-Jurassic Ligurian Tethys ocean during Upper Cretaceous–Eocene times and to subsequent continent–continent collision during the Tertiary (Coward & Dietrich 1989; Dewey *et al.* 1989; Laubscher 1991; Stampfli *et al.* 1998; Schmid & Kissling 2000). Thus, the Apulian plate acted as an indenter with respect to the European plate (Tapponnier 1977). The complex collision history is characterized by the propagation of the compressive front towards external zones. This collision started in Palaeogene times with syn-metamorphic structuring of the internal (Penninic) zones, which consists of a stack of high-temperature (HT) to high-pressure (HP) metamorphic nappes (Dal Piaz *et al.* 1972; Ernst 1973; Goffé & Choppin 1986; Droop *et al.* 1990; Pognante 1991; Spalla *et al.* 1996; Duchêne *et al.* 1997). The metamorphic internal zones overthrusted the external zones along the Penninic frontal thrust during Oligocene times (Butler *et al.* 1986; Choukroune *et al.* 1986; Mugnier & Ménard 1986; Fry 1989; Gratier *et al.* 1989; Butler 1992). The most recent manifestations of collision tectonics are seen in the thin-skinned external fold and thrust belts (Isler 1985; Laubscher 1987; Burkhard 1990; Burkhard & Sommaruga 1998; Schönborn 1999; Becker 2000) which developed in Oligocene (Helvetic chain) to Late Miocene times (Jura, sub-Alpine massifs, southern Alps). At the scale of the western/central Alps, the compressive structures present a fan-shaped pattern, resulting in a near 180° arcuate Alpine chain of 200 to 400 km in width and approximately 1000 km long from eastern Switzerland to the Ligurian margin. The mountain belt is surrounded by peripheral foreland troughs such as the Molasse and Pô basins north and south of the Alps respectively, by Oligo-Miocene rifts such as the Rhine, Bresse and Rhône graben system to the northwest; as well as the Oligocene Ligurian ocean to the southwest. In addition to the dominant and well-studied compressional structures such as nappes, thrusts and folds, extensional structures are now widely recognized to have played an important role in Alpine

*Corresponding author: Université de Neuchâtel, Institut de Géologie, Rue Argand, 11, Case postale 2, CH-2007 Neuchâtel, Switzerland. E-mail: Bastien.Delacou@unine.ch

tectonics since at least Miocene times (Mancktelow 1992; Selverstone *et al.* 1995; Fügenschuh *et al.* 1999; Bistacchi & Massironi 2000; Sue *et al.* 2002; Champagnac *et al.* 2003; Sue & Tricart 2003; Champagnac *et al.* 2004).

While the Alpine structural setting is well constrained, the current tectonic regime and associated geodynamics remain a matter of debate. Instrumental earthquake monitoring began in the Alpine chain in the 1920s (e.g. Rothé 1941; Pavoni 1961; Ahorner *et al.* 1972; Fréchet 1978). The monitoring progressively improved with increasingly more dense seismic networks, so that today more than 74 stations (regrouping French and Swiss networks) are monitoring earthquakes in the central/western Alps (e.g. Pavoni 1980, 1986; Béthoux *et al.* 1988; Ménard 1988; Deichmann & Rybach 1989; Thouvenot *et al.* 1990). The seismicity is considered to be only low to moderate for most parts of the belt (typical magnitude range $3 < M_L < 5$), while a relatively high level of seismicity is found in the southern Valais, the Briançonnais and Piemontais arcs and the southern Rhine graben. Modern seismotectonic studies document the complexity of the present-day tectonic regime. In terms of stress field an orogen-perpendicular orientation of the maximum horizontal compression axis is established along the western periphery of the Alpine chain (Fréchet 1978; Pavoni 1986). In the inner Alpine arc, however, recent surveys have led to the unexpected discovery of an extensional regime (e.g. Maurer *et al.* 1997; Eva *et al.* 1998; Sue *et al.* 1999; Baroux *et al.* 2001; Kastrup *et al.* 2004).

These studies remained rather localized, and no Alpine synthesis has yet been achieved. In this paper we present a seismotectonic synthesis of the entire western/central Alps, leading to a new and comprehensive image of the overall stress state of the belt. The coexistence of extensional, compressional and transcurrent regimes in various areas of the Alps and surroundings still poses unsolved issues. Our synthesis provides a starting point for a discussion of the current geodynamic situation of the Alpine belt. Different scenarios will be discussed in the light of data from neighbouring fields such as geology, geodesy, gravimetry and neotectonics.

2 SEISMOTECTONIC DATA

This study is based on an extensive collection of previously published focal mechanism data, covering the entire arc of the western/central Alps from eastern Switzerland to the Mediterranean sea (Ligurian margin). Our compilation (tabulated in Appendix A) includes all available regional syntheses and local studies for this zone (Ménard 1988; Thouvenot 1996; Eva & Solarino 1998; Sue *et al.* 1999; Baroux *et al.* 2001; Kastrup *et al.* 2004). This database now contains 389 reliable focal mechanisms. The local magnitudes (*Ml*) range from 0.7 to 6.0 for earthquakes recorded between 1969 and 2000 (Fig. 1, see Appendix A). Focal mechanisms have systematically been controlled for their first-arrival polarity and the coherence of their nodal planes (low azimuthal gap and high number of stations) by both previous and present studies (nearly 4 per cent of focal mechanisms were discarded). They can thus be considered as good to very good quality focal solutions.

The complete database has been used to plot the epicentral locations shown in Figs 1 and 2. Cross-sections have been taken from (Schmid & Kissling 2000) and (Calais *et al.* 2000) and earthquakes have been projected vertically onto these sections from a horizontal distance of 25 to 40 km (depending on the density of earthquakes). Note that our catalogue is not a complete catalogue of the seismic activity recorded in the western central Alps, but only presents events for which reliable focal mechanisms are available. Nevertheless, the distribution of the available focal mechanisms provides a fair image of the overall seismic activity of the belt. In comparison with more complete seismic maps of the belt (Thouvenot 1996; Pavoni *et al.* 1997; Béthoux *et al.* 1998; Sue *et al.* 1999; Baer *et al.* 2001), different seismic zones can be distinguished by their relative activity level (Fig. 1): concentrated seismicity occurs in localized zones such as the Basel region, the Valais area and the Piemontais and Briancon-nais arcs (defined in Rothé 1941; Thouvenot 1996; Sue *et al.* 1999); more diffuse seismicity characterizes large zones such as the Swiss Molasse basin, the foreland northwest of the Belledonne massif or the Provence area. Large areas, such as the Vercors or the Lepontin areas, appear as almost aseimic.

Alpine earthquakes occur mainly within the upper crust (the first 15 km), as illustrated by the map and the cross-sections (Fig. 2). However, a few areas with relatively deep seismicity do exist: the Swiss Molasse basin (down to 30 km), the Pô plain (down to 25 km) and the Ligurian margin (down to 20 km). The deep seismicity of the Molasse basin has been interpreted as an indicator of high fluid pressure (Deichmann 1992). In contrast, the seismicity in more internal zones of the belt is restricted to the upper 15 km. It is important to note that informations about present-day stress orientations from focal plane solutions are restricted to this uppermost brittle part of the crust. Any inferences about deeper processes are necessarily indirect and rely on models regarding the coupling between the upper and deeper parts of the orogen.

3 SEISMIC DEFORMATION ANALYSIS

We have used our new database to map regional trends and principal stress orientations as well as to distinguish areas with contrasting stress regimes. In order to constrain the strain state associated with the seismicity, two key parameters have been analysed: the type of deformation (strike-slip, extension, compression) and the directions of P (compressional) and T (extensional) axes of deformation.

3.1 Type of deformation

In order to better visualize the type of deformation derived from focal mechanisms, we used an original approach based on the plunge of P and T axes. Extension is characterized by near vertical P axes, whereas compressional deformation is characterized by near vertical T axes. This qualitative assessment has been used for the calculation of a scalar parameter (see Appendix A), fully sufficient to define the type of deformation, based on assigning negative values of T-axes dips for extensional to transtensional mechanisms and positive values of P-axes dips for compressional to transpressional ones. This 'r' parameter thus ranges linearly from -90 for pure extension to 0 for pure strike-slip and to $+90$ for pure compression. Negative intermediate values indicate a transtensional tectonic regime ($-90 < r < 0$), and positive intermediate values indicate a transpressional tectonic regime ($0 < r < +90$). This approach allows us to interpolate the scalar field of the parameter r, and the corresponding tectonic regime, over the entire area of interest. Such an interpolation (GMT continuous curvature splines in tension, Smith & Wessel 1990) remains open to criticism, as it 'creates' data, as for all interpolation procedures. This is why we also provide the coloured dots on the maps and cross-sections, which correspond to focal mechanisms, with calculated r parameters (see Appendix A). Areas with several dots of the same colour are well constrained by data, while areas in between, especially those with colour gradients and no data points, are filled in purely by interpolation. Different tests have been made in the smoothing procedure (with only minor changes in the resulting maps),

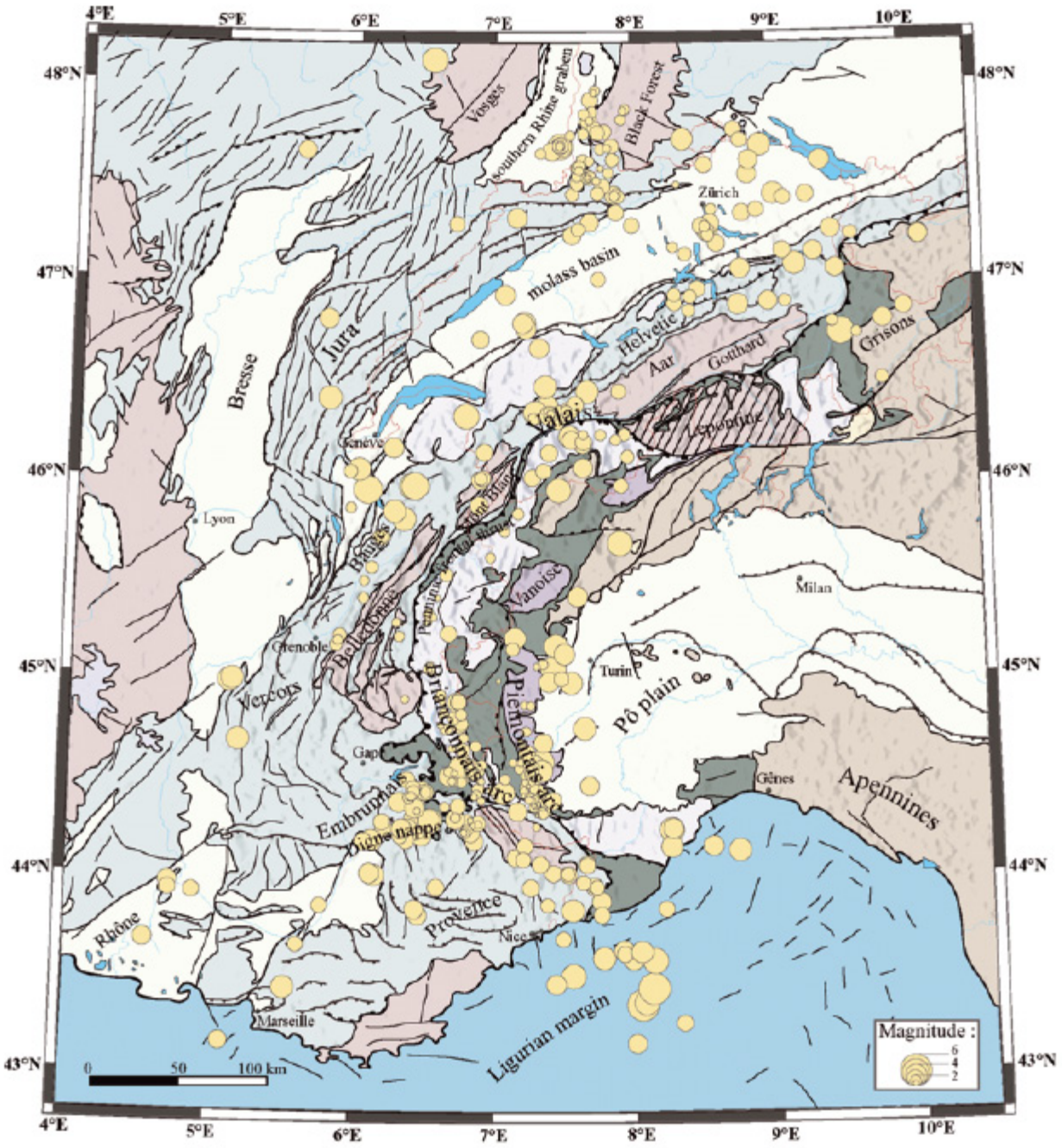

geological caption of Figures 1 and 2

Figure 1. Seismicity map of the western/central Alps showing only the database used in this paper, namely the earthquakes for which a reliable focal mechanism is available. This synthetic database of 389 events recorded between 1969 and 2000 presents the overall features of the classical seismic maps for the Alpine belt: near-aseismic areas (e.g. the Lepontin dome, Vercors), areas of diffuse activity (e.g. Provence, the front of the Belledonne massif, eastern Switzerland) and concentrated active zones (e.g. the so-called Briançonnais and Piemontais arcs, Valais, and the Basel area). The size of the symbols is related to the local magnitude. The geological colour caption is given in the schematic paleogeographical cross-section.

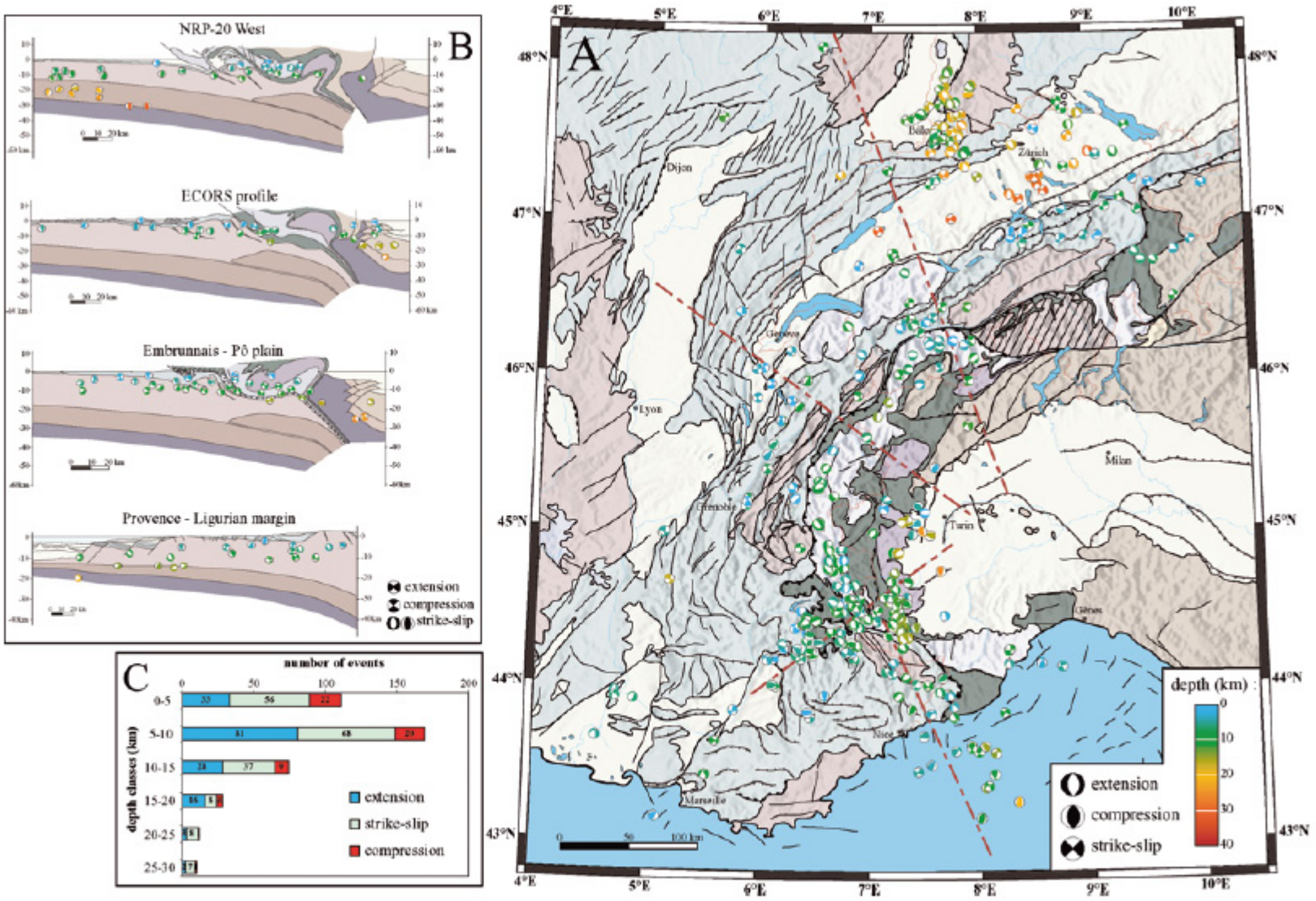

Figure 2. Seismotectonic map of the western Alps (A) showing the whole database used in this study. The colour code of the focal mechanisms corresponds to their depth, and ranges from blue for the shallower ones to red for the deeper ones (up to 35 km beneath the Swiss Molasse basin). The cross-sections (B) are drawn from the recent crustal reinterpretations of the ECORS–CROP and NRP20–West profiles by Schmid & Kissling (2000), and Calais *et al.* (2000) for the Ligurian margin. These key sections illustrate the upper-crustal seismicity in the belt (within the first 15–20 km), and the locally deep seismicity under the forelands. Strike-slip mechanisms are found throughout the whole belt. Reverse faulting is limited to its periphery, whereas extension characterizes the tectonics of the internal zones. The histogram (C) show the depth distribution related to the deformation type for the whole database. See Fig. 1 for the geological caption.

and the parameters have been fixed to reflect the regional patterns and the structural setting of the different areas of interest. Taking into account the limitations inherent in all interpolation methods, our approach allows an accurate assessment of the regional variations of the tectonic regime over the entire western/central Alps (Fig. 3). This approach has its limitations, however, since strike-slip types of deformation (with low r values, corresponding to the green colour code) are obtained not only for the true strike-slip zones (where green dots for strike-slip events are present) but also as an artefact of interpolation between areas of pure extension and pure compression. Nevertheless, this artefact does not hinder compressive and extensive zones to clearly emerge from our interpolation. In summary, our large-scale regionalization approach allows the recognition of large zones with a homogeneous state of deformation and their spatial relationship with regions of contrasting strain regime all along the Alpine arc and the surrounding areas.

The most important feature revealed by the strain regime (Fig. 3) is the emergence of a continuous zone of extension prevalent in the internal zone of the chain, all along the belt from the southern Valais in Switzerland to the north of the Argentera external crystalline massif in southern France. Extension is also found in eastern Switzerland (Grisons area), but without any documented continuity with the western extensional areas. This discontinuity might be an artefact due to a lack of seismicity in the Lepontine dome that separates the extensional domains of Valais and Grisons. Extension has been recognized previously in various regional studies (Fréchet 1978; Roth *et al.* 1992; Maurer *et al.* 1997; Eva *et al.* 1998; Sue 1998; Sue *et al.* 1999; Kastrup *et al.* 2004); here we document a lateral continuity between these areas all along the internal zones of the western central Alps.

Another main feature is the presence of discontinuous transpressive zones localized along the borders of the Alpine belt (Fig. 3). Compression is observed in the eastern Helvetic domain, at the front of the Belledonne massif, in front of the Digne nappe and in the western Pô plain. These zones present only a few compressive focal mechanisms, always associated with strike-slip ones, defining a global transpressive mode of deformation. These compressional/transpressional areas remain very localized in the outer portions of the Alpine realm.

At the margins of the Alpine belt, peripheral systems are interfering with the Alpine system. This is the case for the southern Rhine graben, characterized by a transtensional type of deformation, extending continuously southward to the eastern Swiss Molasse basin in the Zurich region. This is also the case for the Ligurian margin, presenting a clear compressive tectonic regime, extending into the southern Provence area.

3.2 Directional data

Directional informations contained in focal plane mechanisms are visualized through projections of the P- and T-axes orientations on to the horizontal plane (Figs 4 and 5). This directional information is spatially interpolated (Fig. 4) using GMT continuous curvature splines in tension (Smith & Wessel 1990). The resulting maps for P- and T-axes trajectories are shown in Fig. 5. In this representation, P-axis trajectories are shown in transpressional to compressional areas whereas T-axis trajectories are displayed in transtensional to extensional areas (compare Fig. 3).

P-axis trajectories around the bend of the western Alps describe a large-scale fan pattern, convergent towards the Pô Plain, confirming earlier work based on far fewer data (Fréchet 1978; Pavoni 1986). P-axis trajectories are systematically oriented in an orogen-perpendicular fashion, nearly perpendicular to the structural trend of the Alps. The P-axis fan swings of 120° from a NNW direction in eastern Switzerland to northwest in front of Belledonne massif, and southwest in front of the Digne nappe. The Ligurian margin, at the southernmost tip of the belt, is also characterized by horizontal P axis, directed northwest.

T-axis trajectories in internal zones define a radial orogen-perpendicular pattern very similar to the P-axis pattern of the outer Alpine border zones. T-axis trajectories are oriented at a high angle to the bend of the western/central Alpine relief, striking north–south in the Valais to east–west behind the Pelvoux massif area and southwest–northeast behind the Argentera massif. The eastern Swiss Alps (Grisons area) are characterized by T axis striking in a northeast–southwest direction. Thus, the seismic strain documented by these T axis within the internal zone of the Alps is indicating an orogen-perpendicular extensional tectonic regime.

4 STRESS INVERSION

To further characterize the present-day stress state of the western Alps, we applied stress inversion methods to subsets of the focal mechanism database using the software TENSOR (Delvaux 1993). Stress inversion methods assume a uniform state of stress within the study area. Furthermore, in contrast to the inversion of fault-striae data, standard inversion of earthquake data (e.g. Michael 1987; Gephart 1990; Delvaux 1993) does not *a priori* discriminate between the active and the virtual nodal plane. Despite such restrictions, stress inversion has been shown to provide a powerful tool for analysing focal plane mechanism data sets (Larroque *et al.* 1987; Rebaï *et al.* 1992; Delouis *et al.* 1993; Madeddu *et al.* 1996; Maurer *et al.* 1997; Plenefisch & Bonjer 1997; Eva *et al.* 1998; Montone *et al.* 1999; Sue *et al.* 1999; Baroux *et al.* 2001; Kastrup *et al.* 2004). The aim of the inversion of focal plane data is the determination of a regional stress tensor that satisfies most, if not all, observed individual earthquakes in a given area. In contrast to the simple interpolation of isolated, projected P- and T-axes directions (Figs 4 and 5), inversion methods take the entire 3-D orientation of focal plane mechanisms into account and search for a common stress tensor. Our inversion is based on an objective, visual selection of large homogeneous zones, which are characterized by an apparently uniform type of deformation. This selection of zones was based on both Fig. 3, following our regionalization of the r parameter, and Fig. 5, considering the orientation of P and T axes.

Stress inversion was performed for 21 zones (Table 1, Appendix A and B), with 6 to 34 focal mechanisms per zone (18 on average). This very finely divided data set (a high number of stress zones) is required by the extreme curvature of the Alpine arc. As a standard test of the coherence and quality of an inversion procedure, the misfit between the predicted and observed slip direction is calculated for each nodal plane. Average misfit values range from 11° to 27°, with a mean value of 18.8°. These are rather high values, which can be explained by the frequent occurrence of mixed types of focal mechanism (compressional, extensional and/or transcurrent) observed at the local scale. The coexistence of strike-slip focal planes with either extension (internal Alps) or compression (Alpine border) is the rule rather than the exception. Despite this pattern, stress inversion results appear to be fairly robust and reproducible on the regional scale. Our results are very similar to those presented in previous regional studies which used different inversion methods (Michael 1987; Gephart 1990; Delvaux 1993) and different subsets of focal

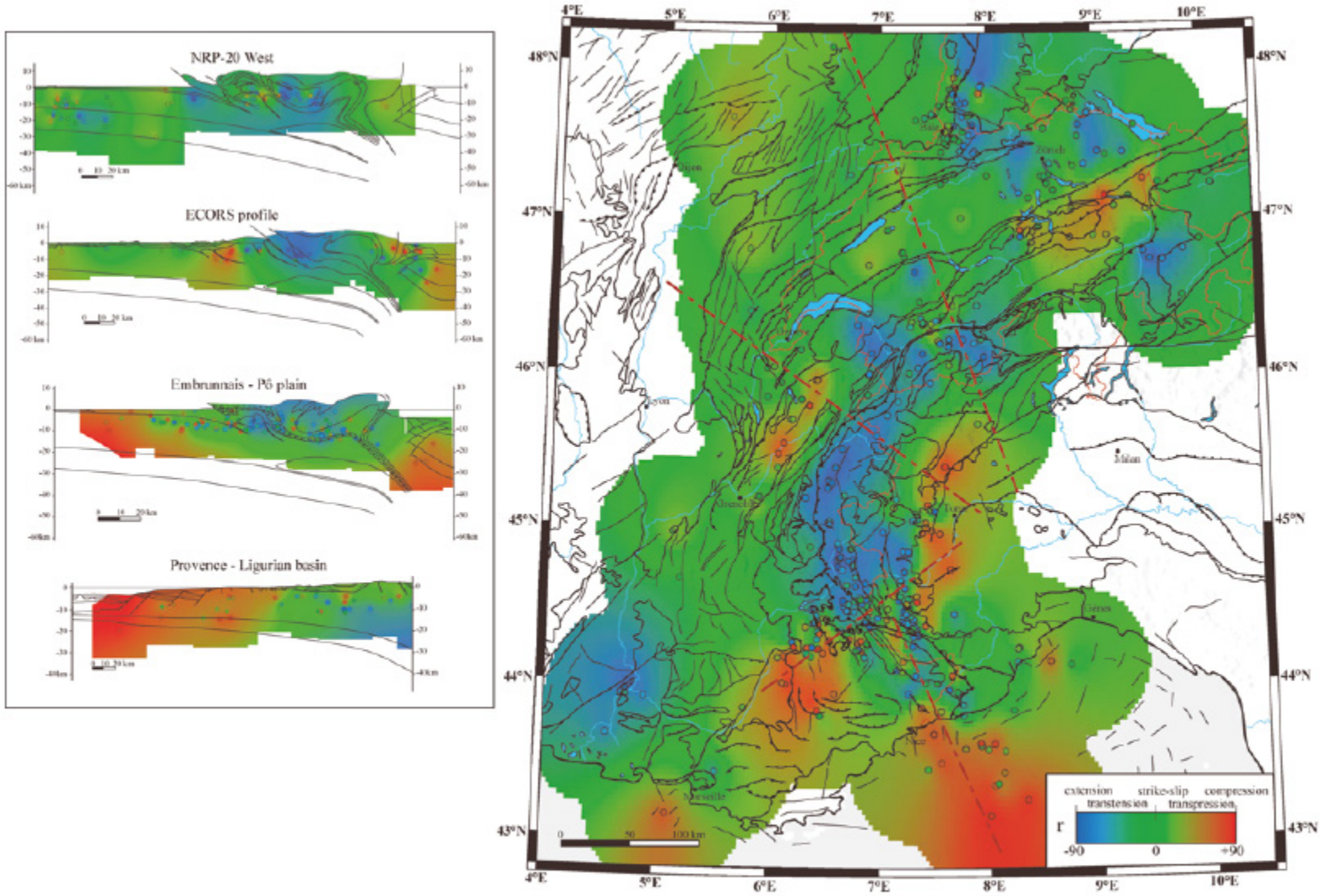

Figure 3. Regionalization of the deformation in the Alpine realm (*r* parameter, based on the *P*/*T*-axes dips, see text) in map and cross-sections. The colour code corresponds to the type of deformation (shortening in red, extension in blue, strike-slip in green). Small circles are observed focal mechanism drawn with their own colour code. The background colour comes from the interpolation of the type of deformation known where focal mechanisms are available. A mask (areas with no colour) is put on areas placed at a distance greater than 55 km from the nearest earthquake. This interpolation shows that extension prevails in the core of the belt, whereas shortening areas remains pretty local and limited to the border of the belt.

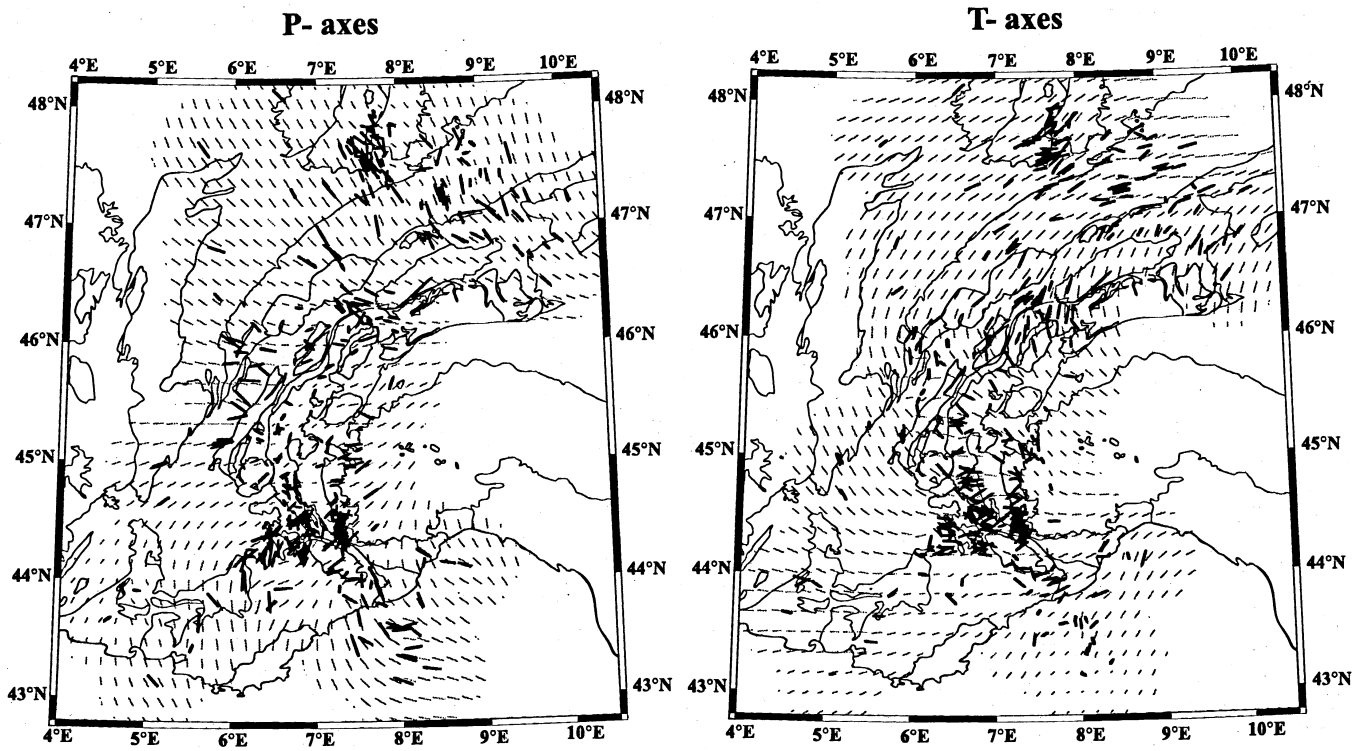

Figure 4. *P*- and *T*-axes fields. Thick lines represent observed *P* (left map) and *T* axes (right map) at the location of focal mechanisms. Thin lines represent interpolated axes. The lengths of axes are inversely proportional to their dips (as projected on the horizontal plane). Note the regionally stable orientation of axes.

plane solutions, such as Maurer *et al.* (1997) for the Valais region, Sue *et al.* (1999) in the southwestern Alps, (Kastrup *et al.* 2004) for all of Switzerland and Baroux *et al.* (2001) in the Provence and Ligurian areas.

Stress inversion results are shown in Fig. 5, together with the interpolated P/T-axes directions. Stress ellipsoids are further characterized by the shape parameter ($\Phi = (\sigma_2 - \sigma_3)/(\sigma_1 - \sigma_3)$), listed in Table 1.

4.1 Internal zones

Orogen-perpendicular extensional stress directions are confirmed and shown to be continuous all along the internal zones, systematically at a high angle to the Penninic frontal thrust (almost perpendicular). The direction of σ_3 varies from N6° in a pure extensive stress state in southern Valais (vss, $\Phi = 0.72$), N119° near radial extension in northern Briançonnais (b1, $\Phi = 0.08$), N91° pure extension in central Briançonnais (b2, $\Phi = 0.50$), N101° transtension in southwestern Briançonnais (b3N, $\Phi = 0.86$) and N53° pure extension in southeastern Briançonnais (b3S, $\Phi = 0.48$). For the Piemontais seismic arc, we also find orogen-perpendicular σ_3 directions with a N131° direction in the north (pieN) and N74° in the south (pieS), both with a nearly pure extensive stress state ($\Phi = 0.56$ and 0.36 respectively). An exception to this overall internal extension is revealed by a few compressive focal mechanisms mixed with extensive ones that have occurred in the southern Piemontais area (Fig. 2). A precise relocation of seismic events recorded in this zone with a dense temporary network (Béthoux *et al.* 2004) show a possible decoupling of the stress state in front of the Ivrea zone, with extension at shallow levels, and compression at depth. This decoupling is not resolved in our large-scale analysis. This is a very complex area with uncertainties in the geometry of the Ivrea body and associated high-pressure tectonic units, as well as in the regional kinematics. Nevertheless, the two types of deformation are analysed independently, following the results of Béthoux *et al.* (2004). We therefore define an independent compressive stress state ($\Phi = 0.22$) in the southern Piemontais zone (pieScomp), with σ_1 oriented N50°.

4.2 External zones

External zones are characterized by contrasted states of stress, with the occurrence of all three possible tectonic modes: strike-slip, extension and compression, according to the zone of investigation (Figs 3 and 4). Generally speaking, strike-slip focal mechanisms dominate in external zones, and lateral variations of tectonic mode to extension (transtension) or compression (transpression) are only locally important. The extensional tectonic mode ranges from pure extensive stress state in northern Provence (pro, $\Phi = 0.63$), eastern Embrunais (diE, $\Phi = 0.76$) and Chamonix areas (cham, $\Phi = 0.43$) to transtensive ones in northeastern Switzerland (zu, $\Phi = 0.92$) and the northern Basel area (balN, $\Phi = 0.92$). Pure strike-slip stress state prevails in northern Valais (vsn, $\Phi = 0.62$). The compressional tectonic mode ranges from pure compressive stress states in the western Pô Plain area (po, $\Phi = 0.4$), the western Embrunais (diW, $\Phi = 0.35$) and the northern Ligurian zone (lig, $\Phi = 0.3$) to transpressive states in front of the Belledonne massif (bel, $\Phi = 0.1$) and eastern Helvetic zones (hel, $\Phi = 0.31$). The front of the Digne nappe (Embrunais) is characterized by a diffuse zone of mixed type of focal mechanisms (compressive, transcurrent and extensive) at the transition between an internal extensive zone and an external compressive one (see Fig. 3). In order to obtain a homogeneous database for the stress inversion, the two types of focal mechanisms (extensive and compressive) have been regrouped independently, resulting in two different stress states (diW and diE zones).

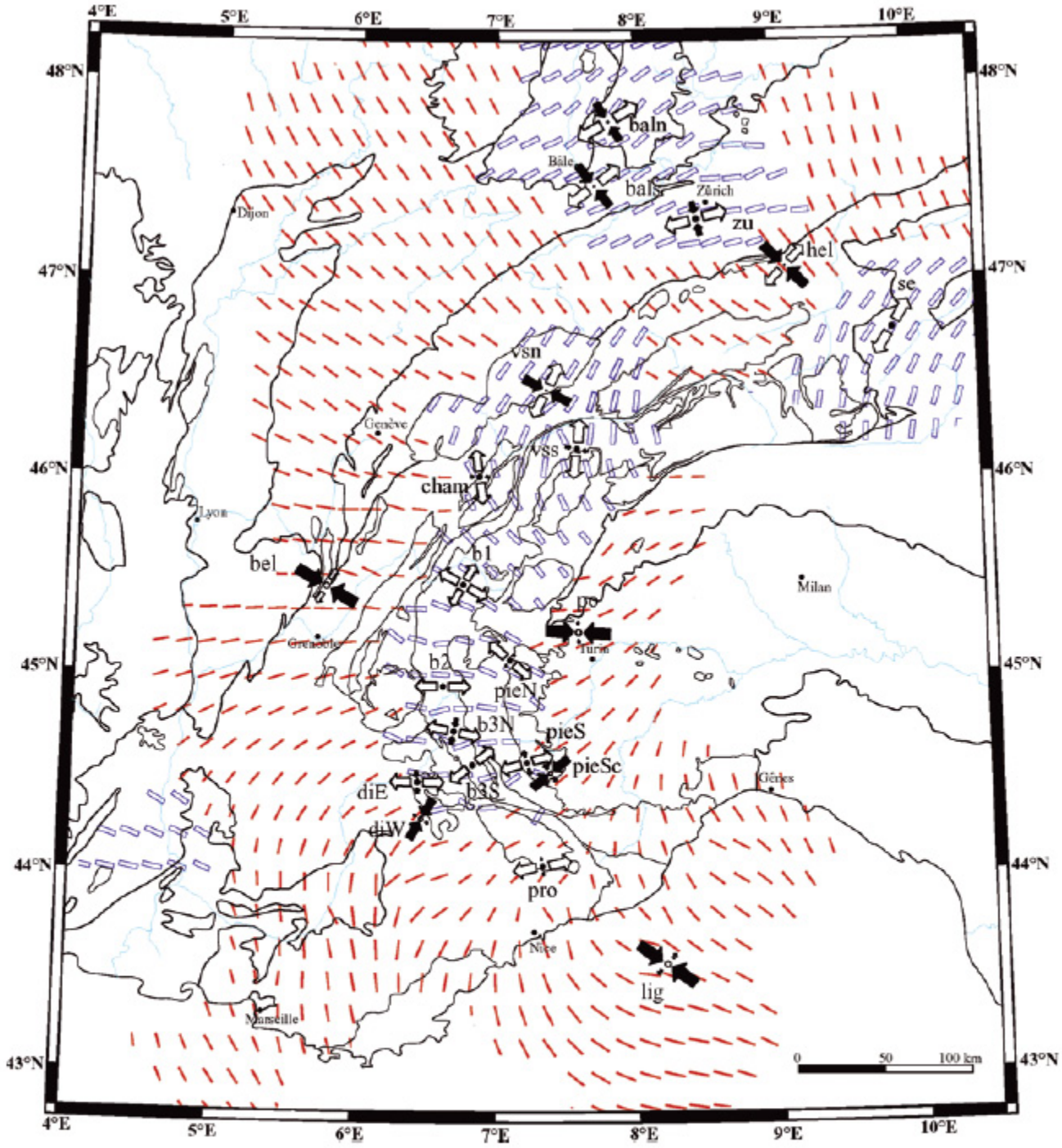

Figure 5. Map of the Alpine strain/stress states. The stress tensors have been inverted in homogeneous areas of deformation determined using the regionalization drawn Fig. 3. Each tensor is presented with the code of the area of inversion (see Table 1 and Appendix B), a black arrow for horizontal σ_1, and an open arrow for horizontal σ_3. The thin red lines correspond to the interpolation of the P axes for transpressive to compressive areas, and the large blue lines correspond to the interpolation of the T axes for transtensive to extensive areas (see Fig. 4).

Despite the complex pattern of stress state at the local/regional scale, large-scale principal stress directions remain coherent all along the external zones, rotating progressively and defining a large-scale radial orogen-perpendicular pattern of σ_1 perpendicular to the belt, from a NNW–SSE direction in northern Switzerland to northwest–southeast in front of Belledonne and southwest–northeast in front of the Digne nappe system.

4.3 Foreland areas

The southern Rhine graben (northern Basel zone, balN) shows a transtensive stress state that continuously extends southeastwards beyond the eastern Jura (balS) and into northern Switzerland (Molass basin, zu), with almost the same σ_1 direction (N140°/160°). The slight differences in the extensive versus transtensive state of

Table 1. Stress tensor parameters. For each stress inversion, the name of the area and the corresponding code (see Fig. 5) are given, with the trend and dip of the principal stress axes σ_1, σ_2, σ_3 (strike, dip). Φ is the shape parameter of the ellipsoid shape, N is the number of focal mechanisms used for the inversion and M is the misfit parameter (average of the differential angles).

Zone	Code	N	σ_1		σ_2		σ_3		Φ	M
			Strike	Dip	Strike	Dip	Strike	Dip		
Northern Valais	vsn	20	118	10	264	78	27	6	0.62	16.81
Grisons	se	6	288	66	122	23	30	5	0.52	11.04
Eastern Helvetic	hel	18	133	1	228	78	43	12	0.31	20.64
Southern Valais	vss	15	253	63	101	24	6	11	0.72	21.71
Chamonix	cham	6	230	55	93	27	352	20	0.43	13.6
Belledonne Front	bel	17	301	1	211	3	50	87	0.1	11.84
Zürich	zu	25	158	59	346	31	254	3	0.92	17.08
Northern Briançonnais	b1	13	340	82	210	5	119	6	0.08	17.27
Western Briançonnais	b2	19	52	85	180	3	271	4	0.5	15.89
Southwestern Briançonnais	b3N	22	194	71	11	19	101	1	0.86	15.94
Southern Briançonnais	b3S	14	335	59	139	30	233	7	0.48	21.86
Eastern Embrunnais	diE	19	12	54	176	35	271	8	0.76	12.16
Western Embrunnais	diW	24	31	3	301	0	206	86	0.35	22.22
Ligure	lig	25	124	13	222	29	13	58	0.3	21.96
Northern Provence	pro	14	160	69	352	21	260	4	0.63	27.31
Basel north	baIN	28	147	39	336	50	240	4	0.92	24.39
Basel south	baIS	31	142	12	355	76	233	8	0.69	18.23
Northern Piemontais	pieN	13	29	87	221	3	131	1	0.56	21.85
Southern Piemontais (ext.)	pieS	34	205	77	343	10	74	8	0.36	23.45
Southern Piemontais (comp.)	pieSc	11	230	7	326	37	130	52	0.22	24.77
Pô Plain	po	9	93	17	356	21	218	63	0.4	15.76

stress can be explained by permutations between the two principal stress axes σ_1 and σ_2, as evidenced by the high Φ ratios computed in these zones (respectively 0.92, 0.69 and 0.92). In contrast, the Ligurian margin is characterized by a pure compressive stress state (lig, $\Phi = 0.3$), with σ_1 oriented N124° perpendicularly to the extensive structures of the Oligocene Ligurian opening. It thus appears that the Ligurian sea is currently reactivated in a compressional tectonic regime (Béthoux *et al.* 1992; Baroux *et al.* 2001).

In summary, the stress field around the arc of the western central Alps is defined as follows: generalized and continuous extension in the core of the belt, with orogen-perpendicular σ_3 axes, contrasting with localized zones of transpression at the outer limits of the belt, in external zones, with σ_1 also perpendicular to the structural trend of the Alpine arc.

5 DISCUSSION

The west European intraplate stresses are characterized by a near spherical ellipsoid of stresses and a consistent N145° ± 26° σ_1/Shmax direction (Zoback *et al.* 1989; Muller *et al.* 1992; Zoback 1992; Golke & Coblentz 1996; Muller *et al.* 1997). This stable σ_1 direction is thought to derive from the Atlantic ridge push, perturbed in a complex fashion in the proximity of the Alps (i.e. within some 300 km around this mountain chain). Numerical modelling by Golke & Coblentz (1996) suggests that the dominant factor responsible for the West European stress field is ridge push, with little or no influence from the Europe/Africa convergence in the Alpine belt. In that case, the West European stress field does not necessarily have to be interpreted in terms of collision processes. However, the near spherical stress ellipsoid allows minor sources of stress to exert a strong influence on the regional to local scale. Thus, the Alpine stress field, with its strong correlation between topography and orogen-perpendicular stress axis trajectories, appears to be largely independent of the far-field European stress fields.

In the following, we will compare the results of our seismotectonic analysis with other geophysical parameters related to the strain/stress states of the Alpine belt.

5.1 Geodesy

On the scale of the western Alps, GPS monitoring puts tight constraints on the permissible present-day displacement vectors between plates and microplates involved in the Europe–Africa collision belt (Calais *et al.* 2002; Nocquet 2002; Oldow *et al.* 2002). While an overall convergence between Africa and Europe is ongoing at rates of 3 to 8 mm yr^{-1} in a general north to northwest direction (Argus *et al.* 1989; Demets *et al.* 1990, 1994; Albarello *et al.* 1995; Crétaux *et al.* 1998; Kreemer & Holt 2001; Nocquet 2002) no clear signal of any relative displacements between northern Italy, eastern France and southern Germany has been detected so far. Given the accuracy of GPS and a limited time span of observation of less than 10 yr, overall Alpine convergence, divergence and/or strike slip movements, if any, have to be less than about 2 mm yr^{-1}.

Within the western Alps, however, 6 yr of continuous GPS monitoring, does indicate some significant displacements (Calais *et al.* 2002; Nocquet 2002). Notably, extension is documented along the Lyon–Turin profile across the western Alps. Along this profile, southeast-directed velocities with increasing strain rates from northwest to southeast, from 0.5 ± 0.9 mm yr^{-1} at La Feclaz (Bauges massif) to 1.7 ± 0.4 mm yr^{-1} at Modane (Vanoise massif), are observed. This results in a lengthening of the Lyon–Modane baseline (along the ECORS–CROP profile) at a rate of 1.4 ± 0.4 mm yr^{-1}. This lengthening correlates very well with the extensional regime documented in our seismotectonic analysis. In the outermost zones of the belt, GPS shows localized zones of convergence, e.g. at the western Pô plain with 1.0 ± 0.5 mm yr^{-1} of east–west to northwest–southeast convergence between Modane and Turin and in the Provence area with 1.4 ± 0.5 mm yr^{-1} of north–south to northwest–southeast shortening between Grasse and Turin. In

summary, GPS results confirm and strengthen the results obtained from seismotectonic investigations, notably the extensional nature of the present-day core of the Alps, apparently compensated by localized compression near the Alpine border.

Additional geodetic information is provided by repeated precise levelling investigations, spanning about 100 yr, available for Switzerland from the Swiss Federal Topographic Office (Gubler *et al.* 1981) and France (see Fourniguet 1977). The Swiss survey has the advantage of covering a large portion of the central Alps including a north–south section across the Gotthard traverse. Furthermore, in contrast to France, where levelling data remain isolated within individual levelling profiles, the entire Swiss levelling data set has been processed so as to provide a coherent picture of the present-day velocity field of vertical movements, with a reference point at Aarberg in central northern Switzerland. With respect to this 'stable' foreland, the entire body of the Alps is rising at a rate of between 1.2 and 1.6 mm yr^{-1}. Maximum velocities are observed in two broad elliptical zones centred in the Valais near Brig-Sion (1.6 mm yr^{-1}) and in the Grisons area (1.4 mm yr^{-1}). In between these two maxima, the Gotthard region appears as a saddle with 'only' about 1.2 mm yr^{-1}. Vertical velocities decrease smoothly northwards and southwards, with isolines running parallel to the general strike of the Alpine chain. Not a single one of the numerous late Alpine faults (post-Miocene) and lineaments which have been crossed by levelling lines shows any indication of tectonic activity within the last 100 yr. This is in stark contrast to the French survey of (Fourniguet 1977), who identified a series of local discontinuities of similar magnitude but barely any regional, large-scale trend when approaching the Alps.

5.2 Deformation versus crustal thickness

5.2.1 Topography

In order to qualitatively examine the relationship between the state of strain/stress and topography we used the GTOPO30 Digital Elevation Model (DEM) database (US Geological Survey EROS Data Center, http://edcdaac.usgs.gov/gtopo30/gtopo30.html). High-frequency topographic features were removed using a smoothing algorithm, calculating at each point the average altitude within a radius of 25 km. This smoothing process provides a proxy for the topographic load, relevant on the scale of the lithosphere, where high average topography is associated (to first order in the western/central Alps) with thickened crust. By smoothing the DEM, we discard high-frequency signals, such as lineaments, or faults. Our purpose was not to correlate the Alpine seismicity with the complex Alpine structures but to study the large-scale relationship between average topography and stress state. Maxima in average topography exist in eastern Switzerland, in the Valais and in the Vanoise areas, whereas more localized and isolated high mountain ranges in external zones, such as the Mont Blanc massif, almost disappeared in our smoothing process. We tested a series of different filters before subjectively choosing the 25 km smoothing radius. Actually, when draping the map of the regionalized deformation (Fig. 3) over the average smoothed Alpine topography (Fig. 6), the high internal areas (the convex crest line of the Alps) appear to very closely match the areas undergoing extensional deformation (eastern Switzerland, southern Valais, Briançonnais and Piemontais arcs). Moreover, transpression very nicely coincides with the negative (concave) curvature at the transition between the Alps and its flat foreland (eastern Helvetic chains, front of the Belledonne massif, western Pô plain, front of the Digne nappe).

5.2.2 Gravimetry

High-resolution gravimetric map have been published recently for the entire western Alpine arc (Masson *et al.* 1999). Internal zones are characterized by strong negative Bouguer anomalies (−160 to −220 mGal), directly related to the thickened Alpine crustal root resulting from the stacking of low-density materials during the Alpine orogenesis. The Bouguer anomaly is closely related to the topography (in the Alpine chain, high topography is generally related to thickened crust), with the exception of the area surrounding the Ivrea body, characterized by a remarkable positive anomaly which is not reflected in topography. This anomaly is classically interpreted as a slab of dense mantle and/or lower crust (Berkhemer 1968; Kissling 1993; Paul *et al.* 2001). Except for the Ivrea body, negative Bouguer anomalies (e.g. zones of high crustal thickness) are closely correlated with internal extensional deformation (Fig. 3) continuously from the Valais to the edge of the Mont Blanc massif, the Vanoise zone and all along the Briançonnais arc (up to the Argentera massif).

In summary, in the western/central Alps as a whole there exists a very close correlation between the generalized Alpine extensional tectonic regime and the zones of high crustal thicknesses (characterized by high large-scale topography and strong negative Bouguer anomalies). This correlation is a strong argument for proposing a geodynamic model in which the current Alpine tectonism is controlled, at least partly, by internal gravitational body forces. In this model, external zones will undergo compression/transpression in response to the balance of gravitational potential energy.

6 MODELS

Several different non-unique geodynamic models can be envisaged in the light of our large-scale seismotectonic analysis and the comparisons previously mentioned.

6.1 Gravitational body forces

Recent studies in the eastern Alps and the adjacent Pannonian basin (Bada *et al.* 2001) using numerical modelling, show that a topography of 1000 to 3000 m can induce 6 to 22 MPa of extensive stress in high zones (eastern Alps relief) and 3 to 12 MPa of compressive stress in the bordering Pannonian basin, contradicting the idea that the relief of the Alps is not high enough to induce significant topographic stresses (Sue *et al.* 1999). Topographically induced stresses would be expected at a high angle to the strike of the belt, as observed in the western Alpine arc (with orogen-perpendicular stresses).

Assuming that large-scale convergent tectonics are negligible in the western Alps (as supported by GPS monitoring, Nocquet 2002), gravitational body forces will tend to equilibrate the mountain belt by balancing the gravitational potential energy between the core of the belt characterized by high crustal thicknesses and its margins. In this case, extensional tectonics are expected within the inner parts of the belt and compressional stresses at the borders. As an isostatic response to this equilibration, uplift is expected in the core of the belt, correlated with negative Bouguer anomalies, as observed in Switzerland (e.g. the Valais and Grisons areas). In terms of isostasy, further complications arise from perturbations induced by Quaternary glaciations, which may have an effect on the rates of vertical uplift and the stress state observed within the upper crust. Simple models of glacial rebound depend strongly on the unknown elastic thickness of the Alpine lithosphere as well as assumed viscosities of the underlying asthenosphere (Gudmundsson 1994). In any case, isostatic rebound effects are expected to correlate with the well-known maximum thickness of glaciers. In Switzerland, two

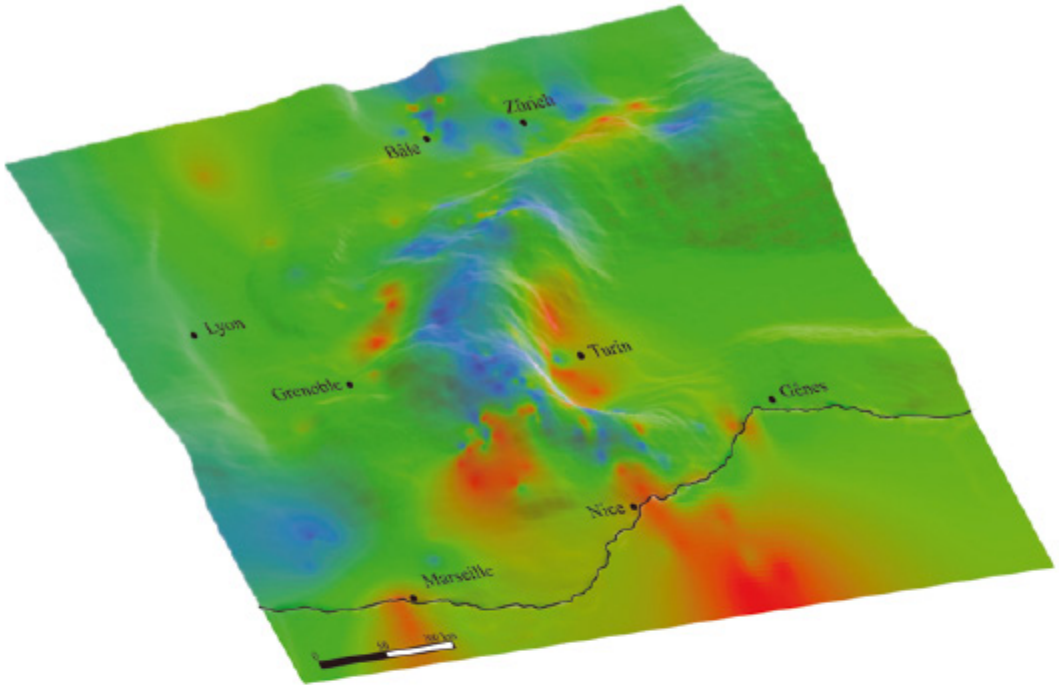

Figure 6. 3-D view of the regionalization of the Alpine deformation. The map of deformation is draped on a smooth digital elevation model (average topography within a radius of 25 km). The continuous extensive zone perfectly correlates with high average topography. Localized external compressive/transpressive zones are located at the bottom of high topographic gradients.

most important ice masses were present in the areas of lakes Geneva and Constance (Jäckli 1962, 1970; Florineth & Schlüchter 1998). Maps of present-day uplift do not exactly reflect this pattern, however, and if present, we think that the effect of glacial rebound on present-day uplift is hidden in the much stronger signal of crustal-scale uplift.

6.2 Rotational models

Geologists have long speculated about the possibility of block rotations between Apulia (African promontory) and Europe as an important factor in the building of the western Alpine arc (Gidon 1974; Anderson & Jackson 1987; Ménard 1988; Vialon *et al.* 1989; Thomas *et al.* 1999; Calais *et al.* 2002). Simple analogue rotation models using sand-box experiments (Collombet 2001; Collombet *et al.* 2002) show great similarities with the Alpine structure: external oblique strike-slip zones, local external thrusting, multiscale arcuate tectonic features. Therefore, rotation models could allow us to explain the large-scale strike-slip mode of deformation, in an overall dextral style, that is observed in external zones (e.g. northern Valais, Mont Blanc/Aiguilles Rouges, front of Belledonne, Briançonnais arc), and that cannot be driven by gravitational body forces. Apulian rotation is further supported by large-scale GPS monitoring regrouping French, Swiss and Italian stations resulting in a microplate anticlockwise rotation of 0.52° Myr^{-1} around a pole located at 45.36°N/9.10°S, near Milan (Calais *et al.* 2002). However, rotation models cannot explain by themselves the overall orogen-perpendicular extension observed on the highest zones of the Alpine belt that is likely to be induced by body forces.

6.3 Proposed model

A combination between gravitational body forces and rotational tectonics could explain most of the current features observed in the western/central Alps. This association, which remains to be quantified, succeeds in explaining the current strain/stress states analysed in this study using seismotectonic tools, namely the generalized orogen-perpendicular extension we characterized in the highest areas of the chain correlated to crustal uplift, the contrasted tectonics between the highest core of the belt and its outer limits in transpression, and the transcurrent part of the Alpine tectonism.

However, the limitations of this analysis (especially in depth) do not permit us to identify the deep deformation processes that could interact in this model. In particular the role of the Ivrea body (moving bloc, passive indenter, etc.) remains unclear. Our impression is that focal mechanism data imply rather consistent deformation with depth. However, improvements in our knowledge of the deep geometry of the Alpine chain would allow us to better define deep tectonic processes.

7 CONCLUSIONS

The compilation of 389 focal mechanisms, all along the Alpine arc and its foreland, allowed us to provide a synthetic and innovative view of the strain/stress states of the western/central Alpine realm as a whole (Fig. 7). The main features of this state of strain/stress are: continuous orogen-perpendicular extension in the inner areas of the belt, and localized zones of compression/transpression at the outer boundaries of the belt, associated with strike-slip areas in external zones, and defining a large-scale fan pattern with orogen-perpendicular σ_1/P axes. Correlations are established between extensional areas and high crustal thicknesses as well as between localized compressive/transpressive areas in external zones and the bottom of high topographic gradients. Moreover, internal extensive zones correlate in its northern part (Switzerland) with areas of maximum crustal uplift (of about 1.6 mm yr^{-1}). In a context of slow horizontal motions (GPS extensional velocities of less than 2 mm

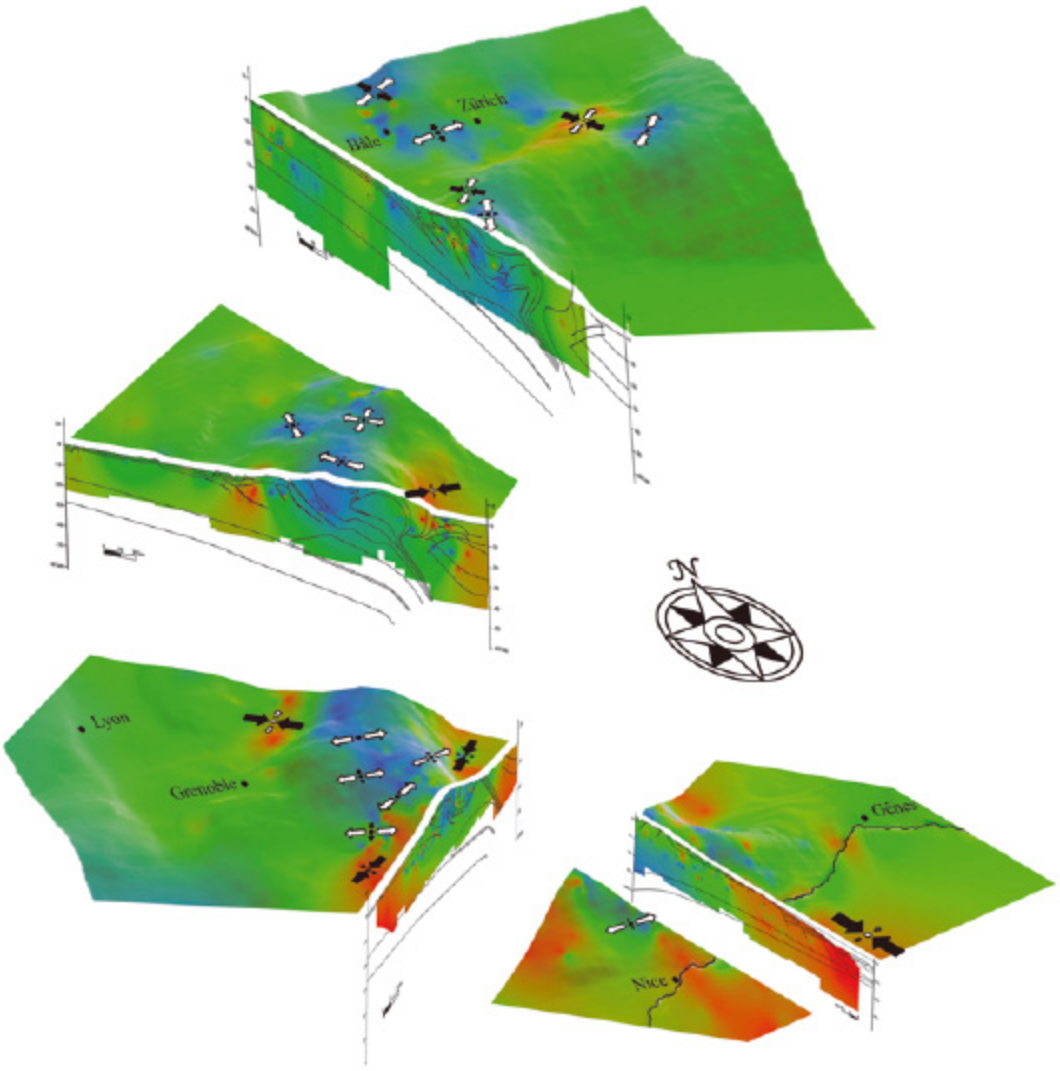

Figure 7. Synthetic 3-D split block of the western Alps showing both the state of stress (inversion) and the deformation state inside the whole belt. The contrasted tectonics between inner and outer areas of the chain and the role of topography and deep structures of the belt are underlined.

yr^{-1} across the whole belt, Calais *et al.* 2002), we propose a model to explain such a strain/stress field combining the following factors: gravitational body forces tending to equilibrate the contrasted gravitational potential energies between the zones of high and low crustal thickness, and large-scale rotational tectonics at the limits of the chain.

Our study addresses the importance of current collisional processes in the realm of the western/central Alps, and more generally the problem of the convergence accommodation between the European and African plates, which should range from 3 to 8 mm yr^{-1} in a north to northwest direction at the longitude of the Alps (Argus *et al.* 1989; Demets *et al.* 1990, 1994; Albarello *et al.* 1995; Crétaux *et al.* 1998; Kreemer & Holt 2001; Nocquet 2002). This convergence could be consumed in different geodynamic areas located between 'stable' Europe and 'stable' Africa such as the Maghrebian belts, the Calabrian subduction, the Apennines, the Dinarides or the eastern Alps. However, in the light of our large-scale seismotectonic study, no direct effect of Europe/Africa convergence can be identified in the western Alpine belt, since the stress field appears to be mostly controlled by internal body forces.

ACKNOWLEDGMENTS

This study was supported by Neuchâtel University and by the Swiss National Science Foundation (grant #21-61684.00). We wish to thank U. Kastrup and N. Béthoux for kindly making their seismological data available, and U. Eichenberger, J. Martinod, M.L. Zoback and D. Hatzfeld for many improvements they brought to the manuscript. Maps were prepared using GMT software (Wessel & Smith 1991).

REFERENCES

Ahorner, Z., Murawski, H. & Scheinder, G., 1972. Sismotektonische Traverse von der Nordsee bis zum Apennin, *Geol. Rundschau,* **61,** 915–942.

Albarello, D., Mantovani, E., Babbucci, D. & Tamburelli, C., 1995. Africa-Eurasia kinematics—main constraints and uncertainties, *Tectonophysics,* **243**(1–2), 25–36.

Anderson, H. & Jackson, J., 1987. Active tectonics in the Adriatic region., *Geophys. J. R. astr. Soc.,* **91,** 937–983.

Argus, D.F., Gordon, R.G., Demets, C. & Stein, S., 1989. Closure of the Africa–Eurasia–North America plate motion circuit and tectonics of the Gloria fault, *J. geophys. Res.*, **94**, 5585–5602.

Bada, G., Horvath, F., Cloetingh, S., Coblentz, D. & Toth, T., 2001. Role of topography-induced gravitational stresses in basin inversion: the case study of the Pannonian basin, *Tectonics*, **20**(3), 343–363.

Baer, M. *et al.*, 2001. Earthquakes in Switzerland and surrounding regions during 2000, *Eclogae Geol. Helv.*, **94**, 253–264.

Baroux, E., Béthoux, N. & Bellier, O., 2001. Analyses of the stress field in southeastern France from earthquake focal mechanisms, *Geophys. J. Int.*, **145**, 336–348.

Becker, A., 2000. The Jura Mountains—an active foreland fold-and-thrust belt?, *Tectonophysics*, **321**(4), 381–406.

Berkhemer, H., 1968. Topographie des Ivrea-Körpers abgeleitet aus seismischen und gravimetrischen Daten, *Schweiz. Mineral. Petrogr. Mitt.*, **48**, 235–246.

Béthoux, N., Cattaneo, M., Delpech, P.Y., Eva, C. & Réhault, J.-P., 1988. Mécanismes au foyer de séismes en mer Ligure et dans le sud des Alpes occidentales: résultats et interprétation, *C. R. Acad. Sci. Paris*, **307**, 71–77.

Béthoux, N., Fréchet, J., Guyoton, F., Thouvenot, F., Cattaneo, M., Eva C., Nicolas, M. & Granet, M., 1992. A closing Ligurian Sea?, *Pageoph*, **139**, 179–194.

Béthoux, N., Ouillon, G. & Nicolas, M., 1998. The instrumental seimicity of the western Alps: spatio-temporal patterns analysed with the wavelet transform, *Geophys. J. Int.*, **135**, 177–194.

Béthoux, N., Sue, C., Paul, A., Virieux, J., Cattaneo, M., Fréchet, J. & Thouvenot, F, 2004. Local tomography and focal mechanisms in the southwestern Alps: comparison of methods and tectonic implications, *Tectonophysics* (in press).

Bistacchi, A. & Massironi, M., 2000. Post-nappe brittle tectonics and kinematic evolution of the north-western Alps: an integrated approach, *Tectonophysics*, **327**(3–4), 267–292.

Burkhard, M., 1990. Aspects of the large-scale Miocene deformation in the most external part of the Swiss Alps (subalpine Molasse to Jura fold belt), *Eclogae Geol. Helv.*, **83**(3), 559–583.

Burkhard, M. & Sommaruga, A., 1998. Evolution of the western Swiss Molasse basin: structural relations with the Alps and the Jura belt, in *Cenozoic Foreland Basins of Western Europe*, Geological Society of London Special Publication 134, pp. 279–298, eds Mascles, A., Puigdefàbregas, C., Luterbacher, H.P. & Fernàndez, M., The Geological Society, London.

Butler, R.W.H., 1992. Thrusting patterns in the NW French Subalpine chains, *Ann. Tecton.*, **6**, 150–172.

Butler, R.W.H., Matthews, S.J. & Parish, M., 1986. The NW external Alpine thrust belt and its implication for the geometry of the western Alpine orogen, in *Alpine Tectonics*, Geological Society of London Special Publication 45, pp. 245–260, eds Coward, M., Dietrich, D. & Park, R.G., The Geological Society, London.

Calais, E. *et al.*, 2000. Crustal strain in the Southern Alps, France, 1948–1998, *Tectonophysics*, **319**(1), 1–17.

Calais, E., Nocquet, J.M., Jouanne, F. & Tardy, M., 2002. Current strain regime in the Western Alps from continuous Global Positioning System measurements, 1996–2001, *Geology*, **30**, 651–654.

Champagnac, J.D., Sue, C., Delacou, B. & Burkhard, M., 2003. Brittle orogen-parallel extension in the internal zones of the Swiss Alps (south Valais), *Eclogae Geol. Helv.*, **96**, 325–338.

Champagnac, J.D., Sue, C., Delacou, B. & Burkhard, M., 2004. Brittle deformation in the inner north-western Alps: from early orogen-parallel extrusion to late orogen-perpindicular collapse, *TerraNova*, doi: 10.1111/j.1365-3121.2004.00555.x.

Choukroune, P., Ballèvre, M., Cobbold, P., Gautier, Y., Merle, O. & Vuichard, J.P., 1986. Deformation and motion in the western alpine arc., *Tectonics*, **5**(2), 215–226.

Collombet, M., 2001. Cinématique et rotation des Alpes occidentales: approche paléomagnétique et modélisation analogique, *Thèse de doctorat*, Université Joseph Fourier, Grenoble.

Collombet, M., Thomas, J.C., Chauvin, A., Tricart, P., Bouillin, J.P. & Gratier, J.P., 2002. Counterclockwise rotation of the western Alps since the Oligocene: new insights from paleomagnetic data, *Tectonics*, **21**, 352–366.

Coward, M. & Dietrich, D., 1989. Alpine tectonics: an overview, in *Alpine Tectonics*, Geological Society of London Special Publication 45, pp. 1–29, eds Coward, M., Dietrich, D. & Park, R., The Geological Society, London.

Crétaux, J.-F., Soudarin, L., Cazenave, A. & Bouillé F., 1998. Present-day tectonic plate motions and crustal deformations from the DORIS space system, *J. geophys. Res.*, **103**, 30 167–30 181.

Dal Piaz, G.V., Hunziker, J. & Martinotti, G., 1972. La zone Sesia-Lanzo e l'evoluzione tettonico-metamorfica delle alpi nordoccidentali interne, *Mem. Soc. Geol. Ital.*, **11**, 433–466.

Deichmann, N., 1992. Structural and rheological implications of lower-crustal earthquakes below northern Switzerland, *Phys. Earth planet. Inter.*, **69**, 270–280.

Deichmann, N. & Rybach, L., 1989. Earthquakes and temperatures in the lower crust below the Northern Alpine Foreland of Switzerland, *Geophys. Monogr.*, **51**(6), 197–213.

Delouis, B., Haessler, H., Cisternas, A. & Rivera, L., 1993. Stress tensor determination in France and neighbouring regions, *Tectonophysics*, **221**, 413–437.

Delvaux, D., 1993. The TENSOR program for reconstruction: examples from the East African and the Baïkal rift systems, *TerraNova*, (abstract suppl. 1), **5**, 216.

Demets, C., Gordon, R.G., Argus, D.F. & Stein, S., 1990. Current plate motions, *Geophys. J. Int.*, **101**, 425–478.

Demets, C., Gordon, R.G., Argus, D.F. & Stein, S., 1994. Effect of recent revisions to the geomagnetic reversal time scale on estimates of current plate motions, *Geophys. Res. Lett.*, **21**, 2191–2194.

Dewey, J.F., Helman, M.L., Turco, E., Hutton, D.W.H. & Knott, S.D., 1989. Kinematics of the western Mediterranean, in *Alpine Tectonics*, Geological Society of London Special Publication 45, pp. 265–283, eds Coward, M., Dietrich, D. & Park, R., The Geological Society, London.

Droop, G.T.R., Lombardo, B. & Pognante, U., 1990. Formation and distribution of eclogite-facies rocks in the Alps, in *Eclogite-facies Rocks*, pp. 225–259, ed. Carswell, D.A., Blackie, Glasgow.

Duchêne, S., Blichert-Toft, J., Luais, B., Télouk, P., Lardeaux, J.M. & Albaréde, F., 1997. The Lu–Hf dating of garnets and the ages of the Alpine high-pressure metamorphism, *Nature*, **387**, 586–589.

Ernst, W.G., 1973. Interpretation synthesis of metamorphism in the Alps, *Geol. Soc. Am. Bull.*, **84**, 2053–2078.

Eva, E. & Solarino, S., 1998. Variations of stress directions in the western Alpine arc, *Geophys. J. Int.*, **135**, 438–448.

Eva, E., Pastore, S. & Deichmann, N., 1998. Evidence for ongoing extensional deformation in the Western Swiss Alps and thrust-faulting in the southwestern Alpine foreland, *J. Geodyn.*, **26**(1), 27–43.

Florineth, D. & Schlüchter, C., 1998. Reconstructing the Last Maximum (LGM) ice surface geometry and flowlines in the Central Swiss Alps, *Eclogae Geol. Helv.*, **91**(3), 391–407.

Fourniguet, J., 1977. Mise en évidence de mouvements néotectoniques actuels verticaux dans le Sud-Est de la France par comparaison de nivellements succesifs, *Rapport BRGM 77SGN081GEO*, Ed, BRGM, Orléans, France, 1–35.

Fréchet, J., 1978. Sismicité du sud-est de la France et une nouvelle méthode de zonage sismique, *Thèse de doctorat d'Etat*, Université des Sciences Technologiques et Médicales, Grenoble.

Fry, M., 1989. Southwestward thrusting and tectonics of the Western Alps, in *Alpine Tectonics*, Geological Society of London Special Publication 45, pp. 83–109, eds Coward, M., Dietrich, D. & Park, R., The Geological Society, London.

Fügenschuh, B., Loprieno, A., Ceriani, S. & Schmid, S., 1999. Structural analysis of the Subbriançonnais and Valais units in the area of Moûtiers (Savoy, Western Alps): paleogeographic and tectonic consequences, *Int. J. Earth Sci.*, **88**, 201–218.

Gephart, J.W., 1990. FMSI: a Fortran program for inverting fault/slickenside and earthquake focal mechanism data to obtain the regional stress tensor, *Comput. Geosci.*, **16**(7), 953–989.

Gidon, M., 1974. L'arc alpin a-t-il une origine tourbillonnaire?, *C. R. Acad. Sci. Paris*, **278**, 21–24.

Goffé, B. & Choppin, C., 1986. High pressure metamorphism in the Western Alps: zoneography of metapelites, chronology and consequences., *Schweiz. Mineral. Petrogr. Mitt.*, **66**, 41–52.

Golke, M. & Coblentz, D., 1996. Origins of the European regional stress field, *Tectonophysics*, **266**(1–4), 11–24.

Gratier, J.P., Ménard, G. & Arpin, R., 1989. Strain-displacement compatibility and retoration of the Chaînes Subalpine of the western Alps, in *Alpine Tectonics*, Geological Society of London Special Publication 45, pp. 65–81, eds Coward, M., Dietrich, D. & Park, R.G., The Geological Society, London.

Gubler, E., Kahle, H.G., Klingele, E., Mueller, S. & Olivier, R., 1981. Recent crustal movements in Switzerland and their geophysical interpretation, *Tectonophysics*, **71**(1–4), 125–152.

Gudmundsson, G.H., 1994. An order-of-magnitude estimate of the current uplift-rates in Switzerland by the Würm Alpine deglaciation, *Eclogae Geol. Helv.*, **87**(2), 545–557.

Isler, A., 1985. *Literatur Zusammenstellung zur Neotektonik/Une Collection Exhaustive de tous les Indices Néotectoniques de Toute la Suisse*, NAGRA International Report 187, NAGRA, Wettingen.

Jäckli, H., 1962. Die Vergletscherung der Schweiz im Würmmaximum, *Eclogae Geol. Helv.*, **55**(2), 285–294.

Jäckli, H., 1970. Die Schweiz zur letzen Eiszeit, Karte 1:550000, *Atlas der Schweiz*, Blatt 6, Office Fédéral de Topographie, Wabern.

Kastrup, U., Zoback, M.L., Deichmann, N., Evans, K. & Giardini, D., 2004. Stress field variations in the Swiss Alps and the northern Alpine foreland derived from inversion of fault plane solutions, *J. geophys. Res.*, **109**(B01402), doi:10.1029/2003JB002550.

Kissling, E., 1993. Deep structure of the Alps: what do we really know?, *Phys. Earth planet. Inter.*, **79**, 87–112.

Kreemer, C. & Holt, W.E., 2001. A no-net-rotation model of present day surface motion, *Geophys. Res. Lett.*, **28**, 4407–4410.

Larroque, J.M., Etchecopar, A. & Philip, H., 1987. Evidence for the permutation of stresses o1 and o2 in the Alpine foreland: the example of the Rhine graben, *Tectonophysics*, **144**, 315–322.

Laubscher, H., 1987. Die tektonische Entwicklung der Nordschweiz, *Eclogae Geol. Helv.*, **80**(2), 287–303.

Laubscher, H., 1991. The arc of the Western Alps today, *Eclogae Geol. Helv.*, **84**(3), 631–659.

Madeddu, B., Béthoux, N. & Stephan, J.-F., 1996. Champ de contrainte postpliocène et déformations récentes dans les Alpes sud-occidentales, *Bull. Soc. Geol. Fr.*, **167**(6), 197–810.

Mancktelow, N.S., 1992. Neogene lateral extension during convergence in the Central Alps: evidence interrelated faulting and backfolding around the Simplonpass (Switzerland), *Tectonophysics*, **215**, 295–317.

Masson, F., Verdun, J., Bayer, R. & Debeglia, N., 1999. Une nouvelle carte gravimétrique des Alpes occidentales et ses conséquences structurales et tectoniques, *C. R. Acad. Sci. Paris*, **329**, 865–871.

Maurer, H., Burkhard, M., Deichmann, N. & Green, G., 1997. Active tectonism in the central Alps: contrasting stress regimes north and south of the Rhone Valley, *TerraNova*, **9**, 91–94.

Ménard, G., 1988. Structure et cinématique d'une chaîne de collision: les Alpes occidentales et centrales, *Thèse de doctorat d'état*, Université Joseph Fourier, Grenoble.

Michael, A.J., 1987. Use of focal mechanisms to determine stress; a control study, *J. geophys. Res.*, **92**(B1), 357–368.

Montone, P., Amato, A. & Pondrelli, S., 1999. Active stress map of Italy, *J. geophys. Res.*, **104**(B11), 25 595–25 610.

Mugnier, J.-L. & Ménard, G., 1986. Le développement du bassin molassique suisse et l'évolution des Alpes externes: un modèle cinématique, *Bull. Centre de Recherche et d'Exploration-Production d'Elf Aquitaine Pau*, **10**, 167–180.

Muller, B., Zoback, M.L., Fuchs, K., Mastin, L., Gregersen, S., Pavoni, N., Stephansson, O. & Ljunggren, C., 1992. Regional patterns of tectonic stress in Europe, *J. geophys. Res.*, **97**(B8), 11 783–11 803.

Muller, B., Wehrle, V., Zeyen, H. & Fuchs, K., 1997. Short-scale variations of tectonic regimes in the western European stress province north of the Alps and Pyrenees, *Tectonophysics*, **275**(1–3), 199–219.

Nicolas, M., Santoire, J.-P. & Delpech, P.-Y., 1990. Intraplate seismicity: new seismotectonic data in Western Europe, *Tectonophysics*, **179**, 27–53.

Nocquet, J.-M., 2002. Mesure de la déformation crustale en Europe occidentale par Géodésie spatiale, *Thèse de doctorat*, Université de Nice.

Oldow, J.S. *et al.*, 2002. Active fragmentation of Adria, the north African promontory, central Mediterranean orogen, *Geology*, **30**, 779–782.

Paul, A., Cattaneo, M., Thouvenot, F., Spallarossa, D., Béthoux, N. & Fréchet, J., 2001. A three-dimensional crustal structure velocity model of the south-western Alps from local earthquake tomography, *J. geophys. Res.*, **106**, 19 367–19 389.

Pavoni, N., 1961. Faltung durch horizontal Verschiebung, *Eclogae Geol. Helv.*, **54**, 515–534.

Pavoni, N., 1980. Crustal stresses inferred from fault-plane solutions of earthquakes and neotectonic deformation in Switzerland, *Rock Mech.*, (Suppl. 9), 63–68.

Pavoni, N., 1986. Regularities in the pattern of major fault zones of the earth and the origin of arcs, in *Origin of Arcs*, pp. 63–78, ed. Wezel, F.C., Elsevier, Amsterdam.

Pavoni, N., Maurer, H.R., Roth, P. & Deichmann, N., 1997. Seismicity and seismotectonics of the Swiss Alps, in *Deep Structure of the Swiss Alps: Results of NRP20*, pp. 241–250, eds Pfiffner, O.A., Lehner, P., Heitzmann, P., Mueller, S. & Steck, A., Birkhäuser, Basel.

Plenefisch, T. & Bonjer, K.P., 1997. The stress field in the Rhine Graben area inferred from earthquake focal mechanisms and estimation of frictional parameters, *Tectonophysics*, **275**(1–3), 71–97.

Pognante, U., 1991. Petrological constraints on the eclogite- and blueschist-facies metamorphism and P–T–t paths in the Western Alps, *J. Metamorphic Geol.*, **9**, 5–17.

Rebaï, S., Philip, H. & Taboada, A., 1992. Modern tectonic stress field in the Mediterranean region: evidence for variation in stress directions at different scales, *Geophys. J. Int.*, **110**, 106–140.

Roth, P., Pavoni, N. & Deichmann, N., 1992. Seismotectonics of the eastern Swiss Alps and evidence for precipitation-induced variations of seimic activity, *Tectonophysics*, **207**, 183–197.

Rothé, J.P., 1941. Les séismes des Alpes Françaises en 1938 et la sismicité des Alpes occidentales, *Ann. Inst. Phys. Globe Strasbourg*, **3**, 1–105.

Schmid, S.M. & Kissling, E., 2000. The arc of the western Alps in the light of geophysical data on deep crustal structure, *Tectonics*, **19**(1), 62–85.

Schönborn, G., 1999. Balancing cross sections with kinematic constraints: the Dolomites (northern Italy), *Tectonics*, **18**(3), 527–545.

Selverstone, J., Axen, G.J. & Bartley, J.M., 1995. Fluid inclusion constraints on the kinematics of footwall uplift beneath the Brenner-line normal fault, Eastern Alps, *Tectonics*, **14**(2), 264–278.

Smith, W.H.F. & Wessel, P., 1990. Gridding with continuous curvature splines in tension, *Geophysics*, **55**, 293–305.

Spalla, M.I., Lardeaux, J.M., Dal Piaz, G.V., Gosso, G. & Messiga, B., 1996. Tectonic significance of Alpine eclogites, *J. Geodyn.*, **21**, 257–285.

Stampfli, G.M., Mosar, J., Marquer, D., Marchant, R., Baudin, T. & Borel, G., 1998. Subduction and obduction processes in the Swiss Alps, *Tectonophysics*, **296**(1–2), 159–204.

Sue, C., 1998. Dynamique actuelle et récente des Alpes occidentales internes—Approche structurale et sismologique, *Thèse de doctorat*, Université Joseph Fourier, Grenoble.

Sue, C. & Tricart, P., 2003. Neogene to current normal faulting in the inner western Alps: a major evolution of the late alpine tectonics, *Tectonics*, **5**, doi: 10.1029/2002TC001426 .

Sue, C., Thouvenot, F., Frechet, J. & Tricart, P., 1999. Widespread extension in the core of the western Alps revealed by earthquake analysis, *J. geophys. Res.*, **104**(B11), 25 611–25 622.

Sue, C., Grasso, J.R., Lahaie, F. & Amitrano, D., 2002. Mechanical behavior of western Alpine structures inferred from statistical analysis of seismicity, *Geophys. Res. Lett.*, **29**(8), 65–69.

Tapponnier, P., 1977. Evolution tectonique du système alpin en Méditerranée: poinçonnement et écrasement rigide-plastique, *Bull. Soc. Geol. Fr.*, **7**, 437–460.

Thomas, J.C., Claudel, M.E., Collombet, M., Tricart, P., Chauvin, A. & Dumont T., 1999. First paleomagnetic data from the sedimentary cover of the French Penninic Alps: evidence for Tertiary counterclockwise rotations in the Western Alps, *Earth planet. Sci. Lett.*, **171**(4), 561–574.

Thouvenot, F., 1996. Aspects géophysiques et structuraux des Alpes occidentales et de trois autres orogénèses (Atlas, Pyrénées, Oural), *Thèse de doctorat d'Etat,* Université Joseph Fourier, Grenoble.

Thouvenot, F., Fréchet, J., Guyoton, F., Guïguet, R. & Jenatton, L., 1990. SISMALP: an automatic phone-interrogated seismic network for the western Alps, *Cah. Cent. Eur. Geodyn. Seismol.*, **1**, 1–10.

Vialon, P., Rochette, P. & Ménard, G., 1989. Indentation and rotation in the Alpine arc, in *Alpine Tectonics,* Geological Society of London Special Publication 45, pp. 329–338, eds Coward, M., Dietrich D. & Park, R., The Geological Society, London.

Wessel, P. & Smith, W.H., 1991. Free software helps map and display data., *EOS, Trans. Am. geophys. Un.*, **72**, 441, 445–446.

Zoback, M.L., 1992. First- and second-order patterns of stress in the lithosphere: the World Stress Map Project, *J. geophys. Res.*, **97**(B8),11 703–11 728.

Zoback, M.L. *et al.*, 1989. Global patterns of tectonics stress, *Nature,* **341**(6240), 291–298.

APPENDIX A: FOCAL MECHANISMS COMPILED IN THE SYNTHETIC DATABASE

Table A1. List and characteristics of focal mechanisms compiled in the synthetic database.

Yr	Mo	Dy	Hr	Mn	Long.	Lat.	Depth	Mag.	Az	Dip	Rake	Az*P*	Dip*P*	Az*T*	Dip*T*	*r*	Zone	Ref.
1968	6	18	05	27.583	7.9000	45.6700	12.0	4.7	240	56	0	200	24	100	25	25	none	M
1970	12	30	02	20.000	8.2530	44.1380	5.0	4.0	224	52	-25	193	42	93	11	−42	none	E
1971	6	21	07	25.000	5.8000	46.4000	3.0	4.4	99	57	−166	315	32	54	14	−32	none	K
1975	1	8	09	12.000	5.7800	46.8000	5.0	3.7	242	70	169	108	7	200	22	22	none	K
1979	4	16	12	27.183	5.1900	44.6700	17.0	4.3	012	60	180	233	22	330	20	−22	none	M
1984	2	19	21	14.628	5.5400	43.4200	8.0	4.3	226	44	−27	204	47	095	17	−47	none	B
1984	4	17	08	53.662	5.1200	44.9700	5.0	4.4	025	90	164	072	14	338	14	14	none	N
1984	4	19	20	41.312	5.1400	44.9800	5.0	4.2	018	84	152	068	15	331	24	24	none	N
1984	12	29	11	2.602	6.5400	48.1100	10.0	4.8	00	89	11	135	07	226	08	08	none	N
1985	11	5	21	35.593	5.6000	47.6500	12.0	3.4	013	63	21	324	05	231	33	33	none	N
1986	2	25	17	10.665	4.7200	43.9500	5.0	3.6	203	43	−78	212	82	105	03	−82	none	B
1987	2	5	9	59.630	4.5600	43.6600	5.0	3.5	356	72	−113	236	57	104	24	−57	none	B
1988	8	5	22	1.554	6.4690	43.7877	5.0	3.6	270	70	−9	228	20	135	08	−20	none	B
1989	4	30	03	38.000	6.7150	47.2820	19.0	2.9	115	61	−156	332	36	66	5	−36	none	K
1992	1	28	21	35.090	5.1043	43.1460	0.5	3.4	250	36	122	137	13	260	67	67	none	B
1996	3	25	4	27.544	4.7263	43.9135	6.0	3.1	190	57	−29	157	42	062	05	−42	none	B
1996	9	26	11	5.672	6.3683	44.8775	6.7	1.5	5	70	−170	227	21	320	7	−21	none	S
1996	10	7	12	26.465	5.7845	43.8335	3.0	2.9	094	67	169	319	09	053	23	23	none	B
1996	11	24	0	27.135	7.6783	44.4450	3.0	3.5	212	27	−45	226	59	089	23	−59	none	B
1997	2	8	19	18.713	5.6228	43.6370	9.0	2.9	050	73	11	004	05	273	19	19	none	B
1998	2	9	14	16.939	4.8913	43.9055	6.0	3.1	024	73	−102	277	60	123	27	−60	none	B
1993	7	21	01	59.272	6.6577	45.5092	3.8	2.4	25	30	−90	115	75	295	15	−75	b1	S
1993	11	22	03	28.905	6.9702	45.5955	6.6	1.8	40	35	−120	205	69	331	13	−69	b1	S
1994	8	1	21	39.438	6.3238	45.1963	1.1	2.1	45	65	−100	295	68	142	19	−68	b1	S
1995	4	21	18	19.517	7.0707	45.7275	13.7	2.1	45	20	−50	75	58	284	29	−58	b1	S
1996	3	31	05	43.134	6.5952	45.3927	8.1	1.2	60	50	−70	35	74	136	3	−74	b1	S
1996	8	1	00	13.047	6.2992	45.2673	2.4	1.7	80	65	−150	299	38	208	1	−38	b1	S
1996	10	25	08	37.133	6.5337	45.3083	7.6	2.0	335	50	−100	192	81	72	5	−81	b1	S
1996	10	28	07	35.518	6.5400	45.2713	8.0	0.8	70	65	−90	340	70	160	20	−70	b1	S
1996	11	5	03	32.343	6.5250	45.2627	8.0	1.2	60	45	−80	56	83	323	0	−83	b1	S
1997	2	19	05	12.897	6.5640	45.2970	6.9	1.5	15	55	−90	285	80	105	10	−80	b1	S
1997	5	15	00	24.064	6.6755	45.2127	9.4	3.1	35	30	−10	15	42	248	33	−42	b1	S
1997	7	14	02	57.936	7.1692	45.8192	14.1	2.2	90	55	−40	60	51	327	2	−51	b1	S
1989	12	13	08	8.227	6.7153	44.7882	9.8	2.3	5	30	−80	69	74	268	15	−74	b2	S
1991	2	11	15	43.713	6.7383	44.8648	6.0	3.8	45	65	−10	5	24	270	11	−24	b2	S
1991	2	13	15	49.650	6.7500	44.8683	3.9	3.0	45	75	−30	1	32	97	9	−32	b2	S
1991	2	13	12	54.704	6.7500	44.8683	5.6	2.8	135	45	−160	341	42	90	19	−42	b2	S
1991	8	12	22	56.152	6.7662	44.8027	2.7	2.2	0	35	−90	90	80	270	10	−80	b2	S
1993	7	10	20	3.983	6.6205	44.8940	2.8	2.2	65	35	−40	61	57	300	19	−57	b2	S
1993	10	30	05	45.205	6.6297	44.7973	5.6	1.2	170	55	−70	131	72	246	8	−72	b2	S
1993	11	10	19	13.288	6.6237	44.7517	8.5	1.4	140	45	−90	301	90	50	0	−90	b2	S
1993	12	14	03	7.120	6.5423	45.0383	7.1	1.9	10	25	−70	61	67	265	21	−67	b2	S
1994	6	18	04	59.971	6.6363	44.8657	9.2	1.2	160	45	−80	156	83	63	0	−83	b2	S
1994	9	17	11	46.998	6.5268	45.0343	8.7	1.5	135	35	−100	262	78	52	10	−78	b2	S
1995	11	22	11	12.878	6.5442	45.0430	8.4	2.1	40	30	−30	36	52	267	26	−52	b2	S
1996	2	18	04	16.551	6.7555	44.7540	9.6	3.3	0	40	−100	147	82	277	5	−82	b2	S
1997	2	21	20	1.752	6.6488	44.8143	9.9	1.9	125	50	−80	88	81	208	5	−81	b2	S
1997	2	21	19	51.549	6.6405	44.8085	8.1	1.8	25	20	−80	98	65	287	25	−65	b2	S
1997	7	19	01	25.708	6.5427	45.0278	9.8	2.0	10	35	−60	25	69	259	13	−69	b2	S
1997	8	3	10	26.424	6.6223	44.9027	7.5	1.8	45	20	−40	64	55	276	31	−55	b2	S
1997	8	30	06	56.607	6.6638	44.7303	8.8	2.2	45	70	−70	344	60	120	22	−60	b2	S
1997	9	13	17	59.648	6.7688	44.7572	8.8	2.6	305	40	−150	142	50	255	18	−50	b2	S

Table A1. (*Continued.*)

Yr	Mo	Dy	Hr	Mn	Long.	Lat.	Depth	Mag.	Az	Dip	Rake	Az*P*	Dip*P*	Az*T*	Dip*T*	*r*	Zone	Ref.
1959	4	5	10	48.000	6.7800	44.5300	0.0	5.3	170	72	−142	34	39	295	11	−39	b3N	E
1977	9	16	18	27.000	6.7848	44.6242	3.1	2.5	6	29	−90	96	74	276	16	−74	b3N	E
1988	3	26	12	17.172	6.6862	44.4912	7.0	3.7	008	56	−123	222	63	121	06	−63	b3N	B
1991	2	7	00	46.907	6.8902	44.4245	9.7	2.3	345	70	−140	208	42	108	11	−42	b3N	S
1991	4	23	05	52.637	6.7173	44.4677	9.8	1.7	95	45	−30	73	49	326	14	−49	b3N	S
1991	11	27	12	18.425	6.8618	44.5240	9.1	1.6	355	50	−110	200	74	99	3	−74	b3N	S
1992	4	11	06	56.862	6.7043	44.4658	9.4	1.6	60	50	−50	37	60	303	2	−60	b3N	S
1993	10	21	15	30.287	6.8777	44.4002	10.6	1.9	60	55	−20	26	37	287	12	−37	b3N	S
1994	2	11	11	35.378	6.9125	44.3682	6.8	1.5	355	45	−110	182	76	279	2	−76	b3N	S
1994	6	22	23	8.599	6.9138	44.5498	11.2	1.8	70	85	−10	25	11	116	3	−11	b3N	S
1994	9	16	17	58.180	6.8715	44.6440	6.1	2.1	160	50	−70	135	74	236	3	−74	b3N	S
1994	9	24	04	18.298	6.8770	44.5363	3.6	2.5	5	70	−110	246	60	110	22	−60	b3N	S
1995	9	11	22	55.888	6.7847	44.6850	5.0	1.9	180	60	−40	145	48	237	2	−48	b3N	S
1995	10	8	06	7.783	6.8955	44.5137	4.8	2.1	10	75	−90	280	60	100	30	−60	b3N	S
1995	10	13	22	7.705	6.8488	44.5113	6.1	2.9	340	70	−140	203	42	103	11	−42	b3N	S
1995	11	17	00	48.739	6.6838	44.5148	8.3	1.8	95	40	−70	108	76	351	7	−76	b3N	S
1995	12	29	02	20.878	6.7205	44.5083	7.9	1.2	95	65	−40	55	45	152	6	−45	b3N	S
1996	6	10	09	2.932	6.8770	44.5338	5.4	1.8	155	65	−90	65	70	245	20	−70	b3N	S
1996	9	9	08	13.402	6.8858	44.4990	10.2	1.0	335	75	−150	199	32	103	9	−32	b3N	S
1996	9	12	08	46.391	6.8262	44.5532	8.8	1.6	345	65	−130	207	52	103	11	−52	b3N	S
1996	12	15	03	56.178	6.8357	44.5383	8.1	1.2	260	80	0	215	7	125	7	7	b3N	S
1996	12	30	11	22.634	6.7030	44.6308	5.4	1.6	80	55	−20	46	37	307	12	−37	b3N	S
1977	9	23	02	41.000	6.8660	44.5327	2.0	2.5	0	22	−57	36	61	245	26	−61	b3S	E
1978	9	30	09	41.000	6.8577	44.5108	7.7	2.5	167	70	−117	293	57	57	20	−57	b3S	E
1980	10	10	21	42.868	7.0700	44.4100	5.0	4.2	128	80	52	9	25	254	42	42	b3S	E
1993	3	22	04	27.046	6.9057	44.4692	8.5	1.6	95	65	150	147	1	56	38	38	b3S	S
1993	6	15	15	0.363	6.8567	44.5213	7.4	1.6	155	70	−90	65	65	245	25	−65	b3S	S
1995	10	18	02	13.158	6.8883	44.5092	4.3	2.1	135	55	−110	354	72	239	8	−72	b3S	S
1996	1	22	16	41.756	6.7720	44.4610	5.4	2.0	5	45	−40	347	55	242	10	−55	b3S	S
1996	8	22	16	14.833	6.9133	44.4677	4.7	1.3	30	70	20	342	1	251	28	28	b3S	S
1996	9	3	01	40.645	6.6710	44.5333	5.4		115	40	−90	205	85	25	5	−85	b3S	S
1996	9	8	17	46.488	6.8625	44.3875	7.8	1.4	150	30	−110	287	71	75	16	−71	b3S	S
1996	10	25	06	13.180	6.8427	44.5120	8.1	1.1	155	35	−60	170	69	44	13	−69	b3S	S
1997	3	1	11	23.335	6.9903	44.4217	10.2	1.7	115	45	−130	309	62	52	7	−62	b3S	S
1997	5	14	17	23.018	7.0803	44.4775	9.1	2.0	200	85	30	330	17	68	24	24	b3S	S
1980	7	15	12	54.000	7.4850	47.6740	10.0	3.7	117	46	−132	314	60	55	6	−60	balN	K
1980	7	15	12	17.000	7.4750	47.6730	12.0	4.7	125	80	174	350	3	81	11	11	balN	K
1980	7	16	15	0.000	7.4810	47.6710	13.0	3.8	201	42	64	129	6	21	72	72	balN	K
1982	10	4	04	6.000	7.8520	47.6740	23.0	2.9	36	74	−6	353	15	261	7	−15	balN	K
1984	6	16	06	43.000	7.8000	47.7500	9.0	2.7	295	41	−118	113	70	225	8	−70	balN	K
1985	2	28	21	33.000	7.4130	47.6500	10.0	3.4	292	49	−169	145	34	250	21	−34	balN	K
1985	9	15	18	18.000	7.7330	47.9540	14.0	2.0	180	44	−33	160	51	52	14	−51	balN	K
1986	1	20	03	48.000	7.7260	47.9450	12.0	1.4	200	40	−48	193	62	81	12	−62	balN	K
1986	10	7	22	23.000	7.9540	47.8600	18.0	2.1	297	42	−114	116	74	224	5	−74	balN	K
1987	7	18	08	59.000	7.4760	47.6730	12.0	2.8	299	80	177	164	5	255	9	9	balN	K
1987	11	21	14	1.000	7.4760	47.6790	12.0	2.8	209	38	64	138	9	18	72	72	balN	K
1988	3	23	21	11.000	7.4740	47.6750	11.0	1.6	7	30	−13	350	44	222	33	−44	balN	K
1988	8	26	00	30.000	7.6880	47.8040	19.0	3.3	307	30	−118	97	67	237	18	−67	balN	K
1988	8	28	20	45.000	7.6940	47.8030	20.0	1.5	296	33	−134	111	61	237	19	−61	balN	K
1988	10	18	11	19.000	7.6480	47.7380	12.0	2.0	272	73	170	138	5	229	19	19	balN	K
1988	11	20	20	43.000	7.5480	47.7300	17.0	1.9	263	68	−177	125	17	220	13	−17	balN	K
1989	3	18	14	26.000	7.6980	47.9090	14.0	3.0	184	27	7	154	36	23	42	42	balN	K
1989	8	12	14	19.000	7.7260	47.7670	19.0	2.7	275	35	−120	80	69	206	13	−69	balN	K
1990	5	11	06	29.000	7.9240	47.8080	20.0	2.0	58	14	56	356	33	193	56	56	balN	K
1990	6	20	10	59.000	7.7130	47.8480	17.0	2.0	31	35	145	263	20	24	54	54	balN	K
1990	7	31	19	13.000	7.7700	47.6590	19.0	2.0	318	21	−109	80	64	243	25	−64	balN	K
1990	12	11	09	10.000	7.9410	47.8530	13.0	1.5	92	35	−132	269	62	32	16	−62	balN	K
1991	1	1	07	29.000	7.6540	47.8360	12.0	2.0	68	63	−176	288	21	25	16	−21	balN	K
1991	5	20	00	13.000	7.8230	47.6640	17.0	1.5	105	73	−170	328	19	59	5	−19	balN	K
1991	8	25	00	6.000	7.3300	47.6380	12.0	2.0	292	76	−172	155	16	247	4	−16	balN	K
1991	11	12	19	10.000	7.4750	47.6790	12.0	1.8	175	59	−22	139	36	44	8	−36	balN	K
1992	12	30	21	34.000	8.3800	47.7100	22.0	4.0	181	71	3	137	11	44	15	15	balN	K
1995	1	10	11	26.000	7.7480	47.7440	14.0	2.7	336	36	−108	126	75	259	10	−75	balN	K
1978	8	13	04	2.000	7.6900	47.2900	24.0	3.4	121	66	−168	341	25	75	8	−25	balS	K
1982	3	25	18	45.000	7.6010	47.4870	7.0	2.5	110	79	−172	334	13	64	2	−13	balS	K

Table A1. (*Continued.*)

Yr	Mo	Dy	Hr	Mn	Long.	Lat.	Depth	Mag.	Az	Dip	Rake	Az*P*	Dip*P*	Az*T*	Dip*T*	*r*	Zone	Ref.
1982	9	3	19	12.000	7.9000	47.4200	11.0	2.5	97	70	−175	319	18	53	10	−18	balS	K
1984	4	10	16	50.000	7.5650	47.4320	22.0	2.6	300	62	−176	160	22	257	17	−22	balS	K
1984	4	12	00	50.000	7.7480	47.4350	21.0	2.5	162	42	−30	143	49	32	17	−49	balS	K
1986	11	1	04	1.000	7.7700	47.5650	19.0	1.2	296	81	−174	160	11	251	2	−11	balS	K
1987	1	8	19	24.000	7.6050	47.2550	6.0	2.6	298	62	−174	158	23	255	16	−23	balS	K
1987	4	11	03	14.000	7.8700	47.4280	7.0	3.4	190	76	−11	146	18	56	2	−18	balS	K
1987	12	11	02	25.000	7.1610	47.3130	9.0	3.7	274	70	168	140	6	232	22	22	balS	K
1987	12	16	09	36.000	7.6750	47.5210	9.0	2.7	6	86	36	134	21	236	28	28	balS	K
1987	12	31	15	16.000	7.6760	47.5180	12.0	1.1	53	40	14	13	26	258	41	41	balS	K
1988	4	16	14	5.000	7.8890	47.4360	9.0	1.9	310	63	−108	187	67	53	16	−67	balS	K
1988	5	11	11	12.000	7.6770	47.5150	10.0	1.5	199	75	−16	156	22	66	0	−22	balS	K
1988	10	27	20	52.000	7.7410	47.5000	12.0	1.6	275	77	−177	139	11	230	7	−11	balS	K
1989	5	5	17	44.000	7.6090	47.5590	10.0	2.2	312	79	−170	176	15	266	1	−15	balS	K
1990	6	16	22	41.000	7.6190	47.5760	18.0	2.0	293	80	177	158	5	249	9	9	balS	K
1990	7	25	14	38.000	7.6720	47.5160	10.0	2.0	180	86	−32	131	25	231	19	−25	balS	K
1990	8	16	18	39.000	7.5990	47.5230	11.0	2.1	282	61	−167	140	29	237	12	−29	balS	K
1990	11	8	19	38.000	7.6980	47.5240	11.0	2.0	282	50	−141	127	53	225	6	−53	balS	K
1990	11	28	01	38.000	7.8300	47.5390	18.0	2.0	319	48	−130	159	61	256	4	−61	balS	K
1991	6	4	17	17.000	7.6140	47.5520	7.0	1.7	360	56	24	311	9	213	39	39	balS	K
1991	11	5	09	13.000	7.6920	47.5990	17.0	1.8	334	43	−122	160	68	266	7	−68	balS	K
1992	3	25	05	33.000	7.6330	47.5150	8.0	2.6	278	65	−160	137	31	230	5	−31	balS	K
1996	4	24	09	36.000	7.6070	47.5650	12.0	2.7	292	55	174	153	20	254	28	28	balS	K
1996	6	15	01	5.000	7.6420	47.6020	21.0	2.4	314	73	165	180	2	271	23	23	balS	K
1996	12	15	04	49.000	7.8860	47.3410	20.0	3.0	313	50	−141	158	53	256	6	−53	balS	K
1997	2	21	05	4.000	7.8750	47.4220	8.0	1.8	316	55	−114	171	69	63	7	−69	balS	K
1997	9	2	00	30.000	7.8610	47.6060	23.0	2.6	128	53	−90	38	82	218	8	−82	balS	K
1999	7	13	20	47.000	7.6960	47.5140	19.0	2.7	215	70	−5	173	17	79	11	−17	balS	K
2000	6	20	06	19.000	7.7870	47.4710	18.0	2.9	111	35	−118	273	70	41	13	−70	balS	K
2000	11	13	16	31.000	7.5600	47.2250	10.0	3.4	90	75	−178	313	12	45	9	−12	balS	K
1975	5	29	00	32.000	6.0200	46.0400	0.0	4.2	242	70	174	106	10	200	18	18	bel	K
1980	12	2	05	58.000	6.2800	45.8300	1.0	4.3	302	76	−4	258	13	167	7	−13	bel	K
1982	11	8	13	2.000	6.2700	46.1500	4.0	3.8	97	62	−167	316	28	52	12	−28	bel	K
1983	11	16	00	27.000	5.9600	46.0300	4.0	2.6	349	90	0	304	0	34	0	0	bel	K
1994	12	14	08	56.000	6.4250	45.9580	10.0	5.1	332	44	29	282	15	173	49	49	bel	K
1996	7	15	00	13.000	6.0880	45.9380	2.0	5.3	316	70	−11	274	22	181	7	−22	bel	K
1994	12	14	08	55.983	6.4090	45.9570	7.0	5.1	220	70	130	281	16	173	49	49	bel	T
1995	4	25	13	2.967	5.9660	45.8450	4.0	2.1	220	85	−169	264	11	354	4	−11	bel	T
1995	9	4	21	1.667	6.1820	45.7000	3.0	2.8	225	70	160	93	1	183	28	28	bel	T
1995	9	4	17	2.900	6.1990	45.7000	11.0	2.9	225	75	160	93	3	181	25	25	bel	T
1995	8	28	12	42.500	6.1190	45.5460	6.0	2.3	25	45	60	315	4	215	69	69	bel	T
1995	12	24	04	5.100	6.0670	45.4760	4.0	1.8	15	45	60	305	4	205	69	69	bel	T
1994	2	4	22	19.783	6.0630	45.3890	7.0	2.0	212	80	164	259	4	168	18	18	bel	T
1995	9	8	16	46.950	5.8990	45.2010	7.0	2.5	45	75	−156	268	18	359	4	−18	bel	T
1994	7	25	00	18.950	5.8850	45.1780	2.0	1.8	215	75	160	263	3	171	25	25	bel	T
1992	3	9	01	54.567	5.8720	45.1540	6.0	2.3	25	70	160	253	1	343	28	28	bel	T
1968	8	19	00	36.683	6.7900	46.3100	9.0	4.8	150	60	−71	098	70	231	09	−70	cham	M
1985	5	25	10	39.951	6.9130	45.9990	4.0	3.0	75	75	81	136	20	25	45	45	cham	E
1986	1	17	07	5.510	6.8952	45.9878	3.0	3.4	50	20	−40	211	55	359	31	−55	cham	E
1988	6	11	22	44.000	6.8860	45.8610	8.0	3.4	34	50	−174	249	31	354	23	−31	cham	K
1988	8	4	10	35.980	6.8978	45.9948	3.0	2.4	40	45	−130	234	62	337	7	−62	cham	E
1999	12	29	09	29.000	6.9230	46.1290	4.0	3.3	111	34	−105	249	76	32	11	−76	cham	K
1986	1	17	20	27.317	6.3960	44.2290	6.0	3.6	010	43	−73	013	78	268	03	−78	diE	B
1986	3	23	13	59.398	6.4400	44.2800	7.0	3.7	140	40	−155	339	47	093	20	−47	diE	B
1987	5	9	6	0.283	6.8650	44.1640	6.0	3.4	050	47	−28	025	47	280	14	−47	diE	B
1990	5	7	14	20.862	6.7480	44.3400	5.0	2.9	255	58	−9	217	28	118	16	−28	diE	B
1990	6	29	8	55.000	6.3420	44.1900	6.0	2.8	018	64	−22	340	33	247	04	−33	diE	B
1992	1	2	02	12.431	6.4352	44.4127	8.3	2.3	50	55	−30	18	44	282	7	−44	diE	S
1992	4	19	22	24.888	6.2155	44.2607	5.0	3.0	121	54	−62	089	67	192	05	−67	diE	B
1992	7	31	20	14.458	6.3883	44.4722	0.5	3.0	035	39	−51	033	64	278	12	−64	diE	B
1994	6	27	17	48.804	6.4328	44.4330	7.2	2.7	165	15	−40	190	53	34	34	−53	diE	S
1994	11	28	08	28.238	6.6562	44.3372	9.2	1.8	15	60	−40	340	48	72	2	−48	diE	S
1996	4	18	05	39.741	6.8903	44.2473	10.0	1.4	5	35	−60	20	69	254	13	−69	diE	S
1996	8	9	17	31.270	6.4180	44.3878	5.9	1.7	350	80	−170	214	14	304	0	−14	diE	S
1996	8	9	18	40.889	6.4025	44.3827	8.7	2.2	345	50	−130	188	60	282	2	−60	diE	S
1996	10	7	02	13.415	6.8093	44.2190	7.9	2.2	175	50	−110	20	74	279	3	−74	diE	S

Table A1. *(Continued.)*

Yr	Mo	Dy	Hr	Mn	Long.	Lat.	Depth	Mag.	Az	Dip	Rake	Az*P*	Dip*P*	Az*T*	Dip*T*	*r*	Zone	Ref.
1996	10	26	16	21.972	6.8013	44.2067	3.4	1.9	25	70	−60	333	55	93	19	−55	diE	S
1996	12	1	11	23.484	6.7923	44.2078	4.7	1.4	15	75	−20	332	25	63	3	−25	diE	S
1997	10	3	15	3.591	6.4440	44.3303	0.5	3.8	037	52	−27	007	43	267	11	−43	diE	B
1997	10	22	04	51.145	6.5215	44.4098	9.1	2.1	20	20	−140	181	55	329	31	−55	diE	S
1969	11	22	07	49.250	6.8060	44.2550	7.0	3.6	166	60	127	231	08	128	58	58	diW	B
1972	6	19	4	9.850	6.3330	44.3600	2.0	3.8	199	60	153	070	05	163	39	39	diW	B
1980	3	15	8	0.798	6.3528	44.2248	5.0	3.8	147	45	124	034	05	135	67	67	diW	B
1983	3	20	16	1.518	6.4500	44.3800	6.0	3.9	010	40	114	263	07	018	73	73	diW	B
1983	12	22	18	12.350	6.7280	44.2750	6.0	3.5	356	57	155	226	08	322	39	39	diW	B
1984	6	19	11	40.618	6.1600	43.9900	10.0	4.1	278	44	109	175	02	276	77	77	diW	B
1984	6	30	19	34.097	6.1300	44.0000	6.0	3.8	300	55	129	003	02	269	59	59	diW	B
1987	5	9	6	0.279	6.8377	44.2050	0.5	3.4	316	43	133	197	10	304	60	60	diW	B
1987	6	28	2	12.881	6.1410	44.1668	1.0	4.0	125	53	118	194	04	095	68	68	diW	B
1989	2	12	3	52.062	6.4930	44.1900	9.0	3.8	302	60	119	012	10	261	63	63	diW	B
1990	6	29	1	19.000	6.3840	44.1670	6.0	3.1	309	86	166	355	07	264	13	13	diW	B
1990	11	9	10	59.043	6.5980	43.9300	2.0	3.3	152	58	55	266	07	008	60	60	diW	B
1993	4	14	10	32.113	6.2272	44.2285	3.0	3.2	134	34	79	052	11	260	77	77	diW	B
1993	5	5	04	34.020	6.8372	44.2683	10.4	1.2	115	25	110	10	21	166	67	67	diW	S
1994	4	15	02	58.218	6.7310	44.2833	6.3	1.8	150	75	−70	85	34	224	63	63	diW	S
1994	11	13	00	36.083	6.4608	44.3180	7.1	1.4	100	70	100	182	24	26	64	64	diW	S
1994	11	24	21	17.590	6.4443	43.8198	1.5	3.5	077	49	77	176	03	285	80	80	diW	B
1996	4	18	05	31.680	6.8898	44.2552	9.7	2.8	65	90	0	20	0	110	0	0	diW	S
1997	10	31	04	23.711	6.5467	44.2710	5.4	4.0	60	60	50	177	7	277	55	55	diW	S
1997	11	6	12	39.799	6.5185	44.4105	8.6	3.1	95	75	30	223	9	319	32	32	diW	S
1998	5	6	12	2.437	6.0858	44.1605	4.0	3.2	166	80	142	221	18	118	34	34	diW	B
1985	9	29	23	36.000	8.3080	46.9220	1.0	2.5	39	26	122	285	22	70	64	64	hel	K
1985	12	21	17	19.000	8.3110	46.8800	2.0	2.9	320	46	−63	307	71	211	2	−71	hel	K
1987	7	26	10	56.000	9.1210	46.8900	1.0	2.4	90	72	144	145	10	47	38	38	hel	K
1987	10	28	23	49.000	9.1960	47.0780	7.0	4.2	178	70	13	132	5	40	23	23	hel	K
1987	11	1	10	16.000	9.6170	47.2250	1.0	2.6	295	78	−169	159	16	249	1	−16	hel	K
1989	4	2	06	58.000	9.1110	47.1440	8.0	3.2	31	43	87	303	2	168	87	87	hel	K
1989	11	19	21	20.000	8.4160	46.8450	6.0	2.4	196	45	8	157	25	47	35	35	hel	K
1990	11	22	15	51.000	8.9990	46.8900	5.0	3.6	341	60	6	298	17	200	24	24	hel	K
1994	8	28	06	4.000	8.7770	46.8750	4.0	3.9	68	56	156	297	9	34	39	39	hel	K
1995	11	16	05	57.000	8.7980	47.0570	4.0	3.8	16	45	0	341	30	231	30	30	hel	K
1996	12	7	05	34.000	8.4250	46.9130	2.0	2.5	172	74	36	297	11	36	37	37	hel	K
1998	4	21	02	30.000	9.3380	47.1400	10.0	3.6	209	78	6	164	4	73	13	13	hel	K
2000	2	23	04	7.000	9.4990	47.0520	7.0	3.6	183	56	18	137	12	38	35	35	hel	K
2000	3	4	15	43.000	9.4700	47.2500	3.0	3.6	235	20	90	145	25	325	65	65	hel	K
2000	6	3	15	14.000	10.1150	47.2140	3.0	3.8	23	57	−12	347	31	247	15	−31	hel	K
2000	6	10	05	51.000	10.1160	47.2120	3.0	3.6	19	53	−13	345	33	243	18	−33	hel	K
2000	8	17	07	14.000	8.4800	46.9540	10.0	3.0	280	80	172	145	1	235	13	13	hel	K
1963	7	19	5	46.067	8.0390	43.3360	14.0	6.0	356	53	60	107	04	205	66	66	lig	B
1963	7	27	5	57.000	8.1300	43.5600	14.0	4.8	000	80	31	129	13	226	28	28	lig	B
1971	9	25	10	34.000	8.7300	44.1170	5.0	4.2	150	75	−11	107	18	016	04	−18	lig	B
1981	1	5	8	10.000	8.0000	43.1410	10.0	3.6	020	50	90	110	05	290	85	85	lig	B
1981	4	22	4	26.350	8.0650	43.3490	9.0	4.5	240	68	0	103	15	197	15	15	lig	B
1985	10	4	15	22.183	7.9160	43.6100	14.0	3.9	210	45	108	107	01	204	77	77	lig	B
1985	10	4	13	17.358	7.9800	43.5700	10.0	4.0	132	66	17	085	06	352	28	28	lig	B
1985	10	5	15	58.667	7.9160	43.5930	11.0	3.1	040	77	159	088	05	356	24	24	lig	B
1986	5	1	00	28.030	7.4400	43.4400	5.0	3.8	115	78	166	341	00	007	17	17	lig	B
1986	10	29	08	13.567	8.2100	43.8210	10.0	3.0	204	84	−9	159	11	250	02	−11	lig	B
1989	12	26	19	59.983	7.5610	43.4830	4.0	4.5	015	60	70	119	13	244	68	68	lig	B
1990	4	15	7	50.600	7.7740	43.5740	5.0	4.3	025	70	42	148	12	259	43	43	lig	B
1990	9	8	8	31.382	7.3800	43.8400	11.0	2.7	060	40	132	301	12	053	61	61	lig	B
1991	2	19	15	33.000	7.6580	44.0430	7.0	3.0	215	40	55	149	10	036	66	66	lig	B
1991	2	25	11	30.197	7.6600	44.0480	4.0	3.3	215	40	53	151	10	038	64	64	lig	B
1991	6	28	23	48.800	7.4900	43.6700	5.0	2.9	092	62	108	169	15	038	68	68	lig	B
1992	9	21	12	37.067	8.3278	43.2445	20.0	3.0	000	50	80	097	05	217	81	81	lig	B
1993	7	17	11	8.387	8.2623	44.2273	9.0	3.7	085	70	−171	307	21	040	07	−21	lig	B
1993	7	17	10	35.010	8.2525	44.2215	7.8	4.5	165	65	10	120	11	25	24	24	lig	E
1995	4	21	8	2.958	7.5563	43.8155	4.0	4.3	030	80	39	155	19	259	35	35	lig	B
1996	11	25	19	47.387	8.5465	44.1390	3.0	3.8	335	40	40	278	14	165	58	58	lig	B
1983	1	22	12	41.950	7.1500	45.1900	5.0	4.1	192	51	−154	041	43	142	12	−43	pieN	N
1984	1	12	08	24.773	7.3500	44.6600	10.0	3.6	5	20	166	215	37	358	46	46	pieN	E

Table A1. *(Continued.)*

Yr	Mo	Dy	Hr	Mn	Long.	Lat.	Depth	Mag.	Az	Dip	Rake	Az*P*	Dip*P*	Az*T*	Dip*T*	*r*	Zone	Ref.
1989	10	30	11	24.095	7.2332	44.6117	9.8	3.0	135	60	−110	4	68	239	13	−68	pieN	S
1989	12	2	08	56.516	7.2277	44.7180	13.6	1.8	120	55	−110	339	72	224	8	−72	pieN	S
1990	1	20	19	25.324	7.1308	45.1347	1.6	2.5	315	90	−140	188	27	82	27	27	pieN	S
1991	7	29	08	46.278	7.2153	44.8510	8.8	1.6	45	25	−60	81	64	293	22	−64	pieN	S
1994	2	9	08	33.383	7.3450	45.0583	15.2	1.8	90	50	−20	60	40	316	16	−40	pieN	S
1995	4	24	00	39.664	7.1958	44.6608	11.4	1.8	10	70	−110	251	60	115	22	−60	pieN	S
1996	10	22	03	39.881	7.0303	44.9755	9.0	0.8	20	60	−110	249	68	124	13	−68	pieN	S
1996	11	3	19	4.203	7.1930	44.6665	10.8	1.1	350	70	−120	222	55	102	19	−55	pieN	S
1996	11	23	10	49.445	7.1927	44.6645	9.4	1.5	170	30	−70	213	71	65	16	−71	pieN	S
1996	12	11	17	50.689	7.2620	44.8483	16.5	1.5	85	45	−60	74	69	334	4	−69	pieN	S
1996	12	16	05	22.622	7.3020	45.0470	16.2	1.4	40	50	−140	245	53	343	6	−53	pieN	S
1971	2	1	12	26.103	7.2600	44.4300	2.0	4.3	150	55	−133	120	56	211	1	−56	pieS	E
1981	1	4	04	9.000	7.3410	44.3280	5.0	3.5	135	70	−50	88	49	197	15	−49	pieS	E
1986	1	17	18	48.050	7.3390	44.3510	6.0	3.3	210	33	−50	219	63	092	17	−63	pieS	B
1986	3	11	07	46.630	7.3200	44.4000	5.0	3.6	247	79	−159	203	23	295	7	−23	pieS	E
1986	7	17	07	35.568	7.2600	44.5300	1.0	3.2	225	45	−140	207	55	102	10	−55	pieS	E
1987	6	15	21	27.302	7.3100	44.4100	10.0	3.3	222	35	−138	44	58	166	18	−58	pieS	E
1992	10	27	03	12.527	7.2428	44.5018	8.7	2.9	140	75	−70	205	56	66	27	−56	pieS	E
1992	11	11	00	59.882	7.2640	44.4847	7.6	2.1	170	45	−80	166	83	73	0	−83	pieS	S
1993	2	15	12	15.046	7.2993	44.3350	11.3	1.9	115	40	−100	262	82	32	5	−82	pieS	S
1993	3	15	23	43.491	7.3235	44.3642	12.3	3.4	110	55	−120	323	65	221	6	−65	pieS	S
1993	4	7	16	36.056	7.2132	44.4185	7.3	1.5	130	75	−100	26	59	228	29	−59	pieS	S
1993	4	10	17	54.425	7.2867	44.4310	14.6	1.8	245	60	−30	210	41	117	3	−41	pieS	S
1994	3	5	08	12.031	7.2238	44.4633	11.4	1.4	130	50	−90	40	85	220	5	−85	pieS	S
1994	9	28	12	43.587	7.3003	44.2363	8.3	1.5	130	55	−110	349	72	234	8	−72	pieS	S
1994	12	7	21	45.618	7.1787	44.5308	12.9	1.8	160	40	−70	173	76	56	7	−76	pieS	S
1995	10	7	19	15.023	7.2803	44.3738	12.5	2.1	10	30	−130	176	62	309	20	−62	pieS	S
1995	10	18	12	52.979	7.3502	44.3028	15.6	1.8	120	45	−100	304	83	37	0	−83	pieS	S
1995	11	24	05	50.275	7.2907	44.3800	15.2	1.6	165	30	−80	229	74	68	15	−74	pieS	S
1996	1	26	01	0.837	7.2583	44.5103	11.9	1.7	335	60	−120	196	62	86	10	−62	pieS	S
1996	1	26	02	19.767	7.2563	44.5043	14.3	2.0	120	35	−130	295	63	58	16	−63	pieS	S
1996	8	9	17	14.630	7.2697	44.4633	9.8	1.4	65	70	−10	23	21	290	7	−21	pieS	S
1996	8	11	08	25.196	7.1908	44.5620	6.9	1.4	325	70	−150	187	35	93	5	−35	pieS	S
1996	8	17	20	5.313	7.2677	44.3692	13.1	1.5	155	50	−100	12	81	252	5	−81	pieS	S
1996	8	23	05	54.655	7.2767	44.4560	11.1	2.0	10	75	−140	236	38	134	15	−38	pieS	S
1996	9	2	00	8.617	7.2533	44.3810	14.9	2.0	125	45	−140	323	55	68	10	−55	pieS	S
1996	9	2	00	17.566	7.2455	44.3753	14.3	1.5	185	30	−80	249	74	88	15	−74	pieS	S
1996	9	11	05	40.641	7.2972	44.3490	12.6	1.9	40	70	−40	357	42	97	11	−42	pieS	S
1996	9	20	22	5.383	7.2592	44.5423	12.2	1.4	345	60	−160	201	34	297	8	−34	pieS	S
1996	10	27	10	11.068	7.2833	44.3442	13.1	0.9	10	50	−110	215	74	114	3	−74	pieS	S
1996	11	3	20	1.406	7.2092	44.3953	11.3	0.8	145	60	−70	96	68	221	13	−68	pieS	S
1996	11	15	23	17.671	7.3070	44.2993	15.5	0.7	170	25	−60	206	64	58	22	−64	pieS	S
1996	11	15	23	35.246	7.3045	44.2990	15.0	1.1	125	50	−130	328	60	62	2	−60	pieS	S
1996	12	12	16	25.964	7.2453	44.4445	12.5	0.9	30	65	−120	257	59	141	15	−59	pieS	S
1996	12	26	19	33.821	7.3038	44.3527	14.9	2.5	335	70	−160	196	28	287	1	−28	pieS	S
1972	12	29	0	14.283	7.1690	44.3140	9.0	3.6	295	48	54	229	03	134	64	64	pieSc	B
1977	2	6	16	1.045	7.3400	44.5200	10.0	4.0	120	48	78	202	2	97	81	81	pieSc	E
1985	2	21	18	0.575	7.4200	44.3700	14.0	3.2	157	65	62	227	15	108	60	60	pieSc	E
1992	11	9	13	11.646	7.3448	44.3137	12.8	1.8	110	70	110	185	22	49	60	60	pieSc	S
1994	1	20	06	59.239	7.3380	44.5612	4.8	4.7	22	75	123	281	20	170	45	45	pieSc	E
1994	1	20	07	5.717	7.2803	44.5473	14.1	4.3	160	75	139	104	15	207	39	39	pieSc	E
1996	8	17	19	29.111	7.2982	44.3528	13.5	1.7	70	90	60	187	38	313	38	38	pieSc	S
1996	9	28	15	48.133	7.1367	44.5628	9.2	1.6	160	85	120	225	33	99	42	42	pieSc	S
1996	11	25	08	39.352	7.2460	44.5110	12.0		40	40	170	258	28	13	38	38	pieSc	S
1996	12	26	19	38.673	7.2908	44.3400	14.0	1.1	350	75	160	38	3	307	25	25	pieSc	S
1996	12	26	19	58.853	7.2830	44.3357	13.5	1.8	270	90	40	37	27	143	27	27	pieSc	S
1980	1	5	14	31.498	7.4190	45.0340	4.0	4.8	215	55	40	92	2	185	51	51	po	E
1981	2	8	04	30.175	7.4390	45.1520	5.0	4.4	155	40	120	266	9	153	69	69	po	E
1981	2	8	04	30.117	7.5000	45.1100	1.0	3.9	100	50	−74	060	78	177	03	−78	po	M
1983	9	6	22	43.307	7.3900	44.9700	5.0	3.8	000	72	75	101	26	249	60	60	po	N
1987	7	3	10	46.951	7.5955	45.3990	3.0	3.7	20	35	80	297	10	147	78	78	po	E
1990	2	11	07	7.797	7.4757	44.9872	24.0	2.7	0	65	120	69	15	313	59	59	po	E
1990	2	11	07	0.630	7.5473	44.9650	16.0	4.2	120	55	120	231	6	333	65	65	po	E
1995	3	4	01	58.230	7.6445	44.7342	25.1	4.3	160	40	60	56	9	162	69	69	po	E
1982	9	2	21	45.417	7.2630	43.9280	10.0	3.3	235	60	−71	185	69	311	13	−69	pro	B

Table A1. (*Continued.*)

Yr	Mo	Dy	Hr	Mn	Long.	Lat.	Depth	Mag.	Az	Dip	Rake	Az*P*	Dip*P*	Az*T*	Dip*T*	*r*	Zone	Ref.
1983	12	4	17	34.850	7.7590	43.8600	4.0	3.5	190	54	−32	160	46	063	07	−46	pro	B
1986	8	18	11	37.200	7.1550	44.0810	6.0	3.2	155	75	−95	065	60	245	30	−60	pro	B
1986	10	20	20	29.183	7.7090	43.9300	2.0	3.0	203	79	−10	159	15	069	01	−15	pro	B
1990	7	2	18	42.000	7.7250	43.9320	4.0	2.7	190	63	−43	152	49	249	06	−49	pro	B
1990	8	9	19	16.960	7.4200	44.0030	6.0	3.2	116	60	−12	078	29	341	13	−29	pro	B
1990	10	2	2	6.402	7.7100	43.9400	11.0	2.9	300	80	−153	165	26	070	11	−26	pro	B
1990	10	22	2	11.147	7.2200	44.1400	4.0	3.0	353	60	−46	053	05	317	52	52	pro	B
1991	2	5	9	6.172	7.7600	43.7900	8.0	3.0	339	75	−44	296	40	037	17	−40	pro	B
1991	7	14	20	47.842	7.2100	44.0700	5.0	2.9	020	81	151	071	13	334	27	27	pro	B
1996	9	26	21	37.612	7.6307	43.9562	7.0	2.7	187	40	−64	194	72	079	08	−72	pro	B
1996	10	17	15	21.646	7.5235	43.9990	11.5	2.5	40	75	−10	357	18	266	4	−18	pro	S
1987	4	29	20	41.000	9.8210	46.4930	8.0	2.6	353	67	−12	312	24	219	8	−24	se	K
1988	4	17	03	41.000	9.4670	46.7830	6.0	2.2	327	43	−59	321	69	216	6	−69	se	K
1988	5	23	21	56.000	9.6420	46.7260	7.0	2.1	345	47	−54	328	64	230	4	−64	se	K
1990	3	18	09	54.000	9.8370	46.7920	4.0	3.5	326	38	−38	317	56	201	17	−56	se	K
1991	11	20	01	54.000	9.5270	46.7310	6.0	5.0	294	37	−72	321	76	191	9	−76	se	K
2000	2	22	22	46.000	9.9940	46.8540	4.0	3.3	174	68	−10	133	22	39	9	−22	se	K
1965	10	24	12	15.937	7.3770	46.3560	10.0	4.4	165	75	−130	115	45	226	20	−45	vsn	E
1967	3	24	17	37.000	7.3630	46.4620	10.0	4.3	265	80	−160	130	21	37	7	−21	vsn	E
1970	8	18	04	25.528	7.6690	46.4370	10.0	4.2	160	60	2	119	19	20	22	22	vsn	E
1979	7	3	21	13.000	7.0720	46.9250	30.0	3.8	285	86	179	150	2	240	4	4	vsn	K
1981	9	26	13	54.768	7.2900	46.3300	5.0	4.4	189	83	23	321	11	55	21	21	vsn	E
1986	10	9	10	8.000	7.4720	46.3190	4.0	3.6	79	61	167	304	12	41	28	28	vsn	K
1987	9	20	11	53.000	7.2200	46.7560	9.0	3.9	7	81	0	323	6	232	6	6	vsn	K
1988	10	14	19	2.000	6.8890	46.6980	2.0	3.3	350	69	20	302	2	211	29	29	vsn	K
1989	1	7	02	29.000	7.5390	46.3420	4.0	3.4	57	68	170	282	9	16	22	22	vsn	K
1989	9	30	04	41.000	7.3940	46.3170	6.0	3.5	110	90	140	163	27	57	27	27	vsn	K
1990	4	28	22	24.000	7.5160	46.3370	3.0	2.2	266	46	−145	108	52	212	11	−52	vsn	K
1990	5	7	16	6.000	7.4040	46.3230	7.0	1.6	175	45	−31	153	49	46	14	−49	vsn	K
1990	6	3	19	23.000	7.2820	46.2980	3.0	2.2	100	60	−151	315	41	48	3	−41	vsn	K
1990	7	26	12	30.000	7.3950	46.3250	7.0	2.4	285	80	−140	154	35	50	19	−35	vsn	K
1990	8	31	10	57.000	7.4580	46.2710	7.0	2.0	181	53	25	132	11	32	42	42	vsn	K
1995	9	17	16	29.000	7.2000	46.7820	10.0	3.8	175	88	3	310	1	40	4	4	vsn	K
1996	2	21	18	57.000	7.5790	46.3680	5.0	3.3	242	87	−178	107	4	197	1	−4	vsn	K
1997	11	28	08	30.000	7.8980	46.4370	12.0	2.9	250	60	−150	105	41	198	3	−41	vsn	K
1999	2	14	05	58.000	7.2120	46.7820	10.0	4.3	354	88	9	129	5	219	8	8	vsn	K
1999	5	20	13	11.000	7.3200	46.6550	7.0	3.8	300	42	−82	326	84	204	3	−84	vsn	K
1968	7	8	05	45.582	7.5400	46.2100	5.0	4.0	79	58	156	30	8	294	38	38	vss	E
1985	1	4	16	57.000	7.2690	46.0020	10.0	3.2	329	82	−40	279	33	23	21	−33	vss	K
1986	1	19	06	54.000	7.6400	46.1830	6.0	3.0	110	40	−80	143	82	13	5	−82	vss	K
1986	2	15	01	43.000	7.6380	46.0510	5.0	3.6	27	70	170	252	7	345	21	21	vss	K
1986	2	26	13	7.000	7.3500	46.0340	7.0	2.9	249	51	−133	94	58	188	2	−58	vss	K
1986	6	9	17	58.649	7.9578	46.1063	10.0	2.6	60	35	−80	113	78	323	10	−78	vss	E
1987	3	22	01	36.000	7.8720	46.1920	4.0	2.1	311	51	−47	286	58	192	2	−58	vss	K
1987	5	30	19	45.000	7.9090	45.9610	9.0	2.7	135	50	−10	101	33	357	21	−33	vss	K
1990	5	11	08	16.000	7.7650	46.2180	1.0	2.0	263	40	−116	76	72	191	8	−72	vss	K
1990	9	25	05	19.000	7.6350	46.1730	5.0	3.6	70	50	−130	273	60	7	2	−60	vss	K
1990	12	17	23	34.000	7.6380	46.2190	5.0	1.7	319	42	−49	310	62	201	10	−62	vss	K
1991	9	7	18	9.000	7.9370	46.2190	8.0	2.4	135	55	−19	101	37	2	12	−37	vss	K
1996	3	31	06	8.000	7.4600	45.9380	4.0	4.6	44	38	−137	231	59	347	15	−59	vss	K
1998	5	7	17	16.000	7.3930	46.1260	6.0	3.3	92	55	−90	2	80	182	10	−80	vss	K
1998	12	9	22	8.000	7.5520	46.1910	4.0	3.4	256	28	−80	323	72	159	17	−72	vss	K
1976	3	2	08	27.000	9.4000	47.6000	10.0	3.7	31	90	0	346	0	76	0	0	zu	K
1977	11	21	19	27.000	8.5800	47.2800	25.0	3.5	33	80	−5	349	11	258	4	−11	zu	K
1978	8	28	14	44.000	8.9200	47.3500	22.0	2.8	9	40	−46	1	60	249	12	−60	zu	K
1979	11	30	00	44.000	8.5100	47.2700	27.0	3.1	296	84	−176	161	7	251	1	−7	zu	K
1983	9	4	21	51.000	8.8070	47.7030	8.0	2.8	159	74	175	24	8	116	15	15	zu	K
1984	1	11	14	11.000	8.8150	47.3350	11.0	3.2	36	76	5	351	6	259	13	13	zu	K
1984	9	5	05	16.000	8.5620	47.2470	15.0	4.0	8	44	−26	345	46	236	17	−46	zu	K
1984	9	14	22	30.000	8.5570	47.2430	24.0	2.9	315	67	−158	175	31	266	2	−31	zu	K
1985	1	7	09	52.000	8.3030	47.1620	27.0	2.1	336	46	−125	170	65	270	4	−65	zu	K
1985	7	7	00	8.000	7.7530	47.0030	30.0	2.7	124	80	169	170	1	80	15	15	zu	K
1986	2	27	12	7.000	8.9550	47.6800	17.0	4.2	304	38	−138	131	58	247	15	−58	zu	K
1986	10	8	03	12.000	8.5420	47.2670	28.0	2.0	315	66	−160	174	30	267	4	−30	zu	K
1987	1	29	00	7.000	9.2870	47.4260	8.0	3.2	10	45	−54	357	65	255	6	−65	zu	K

Table A1. (*Continued.*)

Yr	Mo	Dy	Hr	Mn	Long.	Lat.	Depth	Mag.	Az	Dip	Rake	Az*P*	Dip*P*	Az*T*	Dip*T*	*r*	Zone	Ref.
1987	5	5	20	29.000	8.5640	47.2250	29.0	2.3	304	75	−170	167	18	258	4	−18	zu	K
1988	9	11	23	1.000	8.3900	47.1300	29.0	2.5	298	74	180	162	11	254	11	11	zu	K
1989	2	21	23	36.000	8.8580	47.5310	22.0	3.5	273	62	−165	131	30	227	10	−30	zu	K
1989	6	9	01	30.000	8.3310	47.4780	18.0	1.3	142	42	−105	311	79	63	4	−79	zu	K
1989	10	24	12	3.000	8.5910	47.3530	12.0	2.1	314	30	−166	150	44	278	32	−44	zu	K
1990	1	5	04	21.000	9.1230	47.4120	5.0	2.9	126	78	−160	350	23	258	5	−23	zu	K
1990	8	11	05	31.000	8.0000	47.2740	15.0	2.8	11	90	0	326	0	236	0	0	zu	K
1995	6	25	18	53.000	8.8730	47.6040	12.0	3.5	167	58	−90	77	77	257	13	−77	zu	K
1996	6	28	03	43.000	8.7610	47.7590	9.0	3.1	289	78	−172	153	14	244	3	−14	zu	K
1996	8	24	02	38.000	9.0490	47.4320	29.0	4.0	184	42	−63	183	72	75	6	−72	zu	K
1997	10	23	12	7.000	8.6240	47.1810	30.0	3.2	221	65	−2	179	19	84	16	−19	zu	K
1999	9	12	13	25.000	8.5380	47.5800	2.0	3.1	151	80	175	16	3	107	11	11	zu	K

Yr, year; Mo, month; Dy, day; Hr, hours; Mn, minutes and seconds; Long., longitude; Lat., latitude; Mag., magnitude (M_L); Az, azimuth of fault plane; Dip, dip of fault plane; Rake, rake of fault plane solution; Az*P*(*T*), azimuth of *P*(*T*) axes; Dip*P*(*T*), dip of *P*(*T*) axes; *r*, parameter defining the type of deformation (see Fig. 3; Zone, associated stress inversion zone; Ref., reference (B, Baroux *et al.* (2001); E, Eva & Solarino (1998); K, Kastrup *et al.* (2004); M, Ménard (1988); N, Nicolas *et al.* (1990); S, Sue *et al.* (1999); T, Thouvenot (1996)).

APPENDIX B:

Stereograms of inverted stress tensors and associated focal planes used for the inversion. Inside the stereograms: circles are σ_1 principal stress axes; squares σ_2 axes; triangles σ_3 axes. Outside the stereograms: black arrows represent the horizontal direction of compression and open arrows the direction of extension. The size of the arrows is a function of the Φ ratio of the ellipsoid shape.

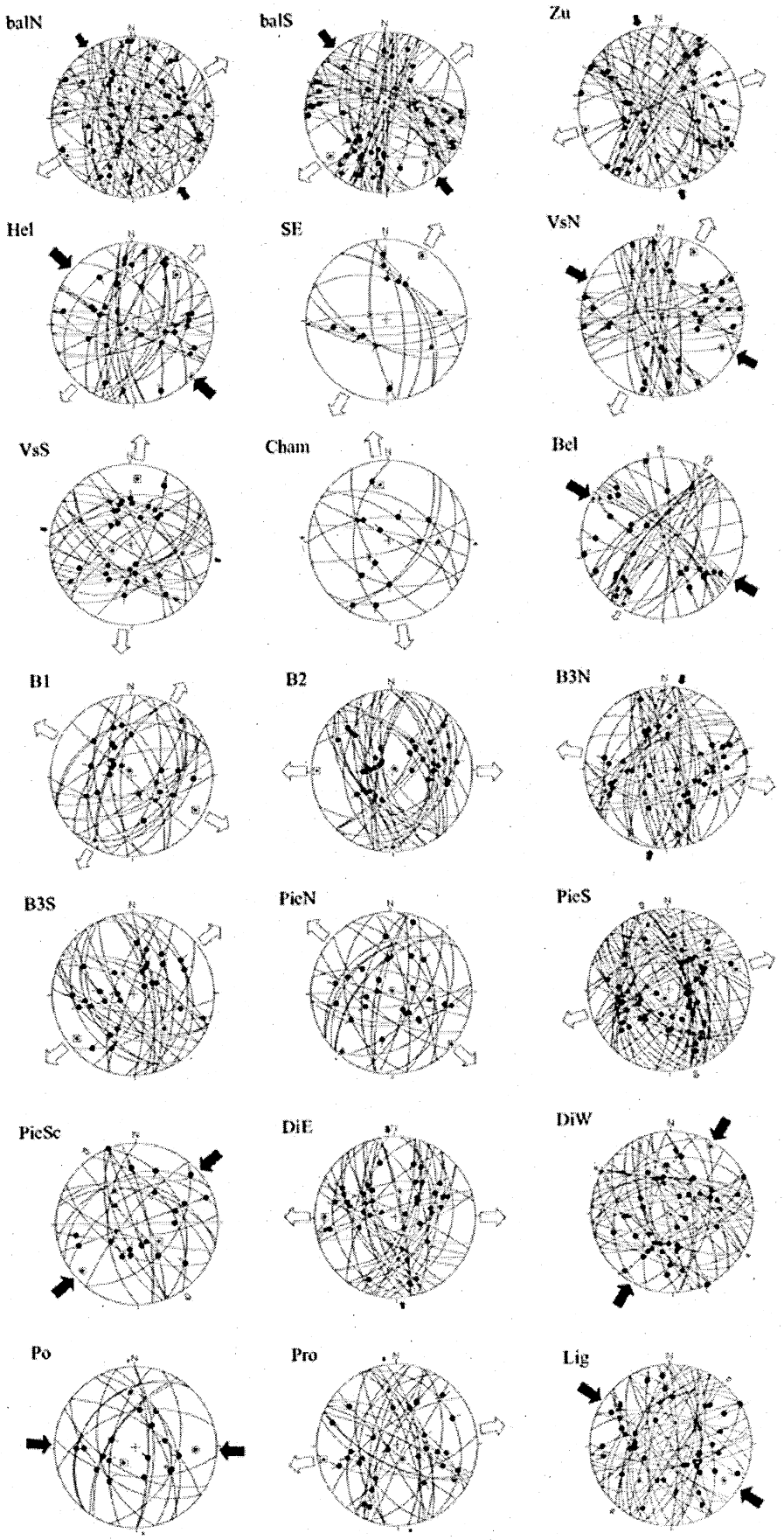
balN
balS
Zu
Hel
SE
VsN
VsS
Cham
Bel
B1
B2
B3N
B3S
PieN
PieS
PieSc
DiE
DiW
Po
Pro
Lig

Figure B1.